Electrodeposition of palladium in H_2O and D_2O

Master's Thesis
University of Turku
Department of Mechanical and Materials Engineering
Materials Engineering
2022
Kimmo Pyyhtiä

Reviewed by:
Pekka Peljo

The originality of this thesis has been checked in accordance with the University of Turku quality assurance system using Turnitin OriginalityCheck service.

UNIVERSITY OF TURKU
Department of Mechanical and Materials Engineering
PYYHTIÄ, KIMMO TAPIO Electrodeposition of palladium in H_2O and D_2O
Master's Thesis, 51 pages, 8 appendixes
Materials Engineering
February 2022

In this Master's thesis the electrodeposition of palladium on pencil graphite in aqueous solutions of either H_2O or D_2O at different acidities was examined experimentally utilizing chronoamperometry and cyclic voltammetry. Electrochemical cells and their theory was examined along with how electrochemical reactions occur on the electrode surfaces. Based on the experiments the nucleation process was observed to follow progressive nucleation mechanism as described by Scharifker-Hills theory. Current profiles from chronoamperometric measurements followed the theoretical description by Heerman and Tarallo and values for nucleation constant per site, number density of active sites and diffusion coefficients were obtained for each sample solution. Overall the effects of using D_2O instead of H_2O had only small effects on these values and should be examined in further experiments more thoroughly.

Keywords: electrodeposition, palladium, graphite, deuterium, nucleation, instantaneous, progressive

Contents

Introduction

Electrochemical systems can be found in almost every industry and is a mainstay medical, material and biological sciences. It is a powerful tool for diagnostics, refining ores and myriad of different chemical analysis. In this Master's thesis the theory of electrochemistry is presented and is then used to examine the nucleation process of palladium on pencil graphite to learn how the system behaves using light and heavy water as the solvents. The results are then then compared to literary sources and and based on those conclusions on the nucleation process and parameters derived from the processes are drawn.

Palladium, as a noble metal belonging to the platinum group, is an interesting metal for its ability to catalyze hydrocarbons and one of its most widely used applications is in the catalyzers of cars converting carbon monoxide to less harmful carbon dioxide and oxidizing unburnt hydrocarbons into carbon dioxide and water. Thus the study of palladium and it's use in electrochemistry is important to optimize its use and find new uses or ways to manufacture palladium in different forms, such as in nanoparticles.

1 Electrochemistry basics

Study of redox active species, their chemical reactions and transport in system consisting of the charged particles, their medium and an external circuit is known as electrochemistry. The charged particles, which can be ions, ion complexes or larger molecules, are suspended in an electrolyte of a salt and a solvent, most often water. In addition to a solvent and charged particles the system also has electrodes. The purpose of the electrodes is to enable electrochemical reactions as those occur only on interfaces and not in the bulk electrolyte separating electrochemical reactions from normal chemical reactions where reactions would take place in the entire solution. The electrodes are connected to each other via an external circuit allowing current to flow between the electrodes. Both potential difference and current can be measured, and also controlled with a power supply on a load. The total system consisting of an electrolyte, electrodes and an external circuit is known as an electrochemical cell [1].

Electrochemical reactions always include the transfer of electrons between redox active species and electrode. A particle can give one or more of its electrons in which case the reaction is called oxidation. If a particle receives electrons then the reaction is known as reduction. Oxidation and reduction are two half-reactions that are present in every electrochemical cell [1].

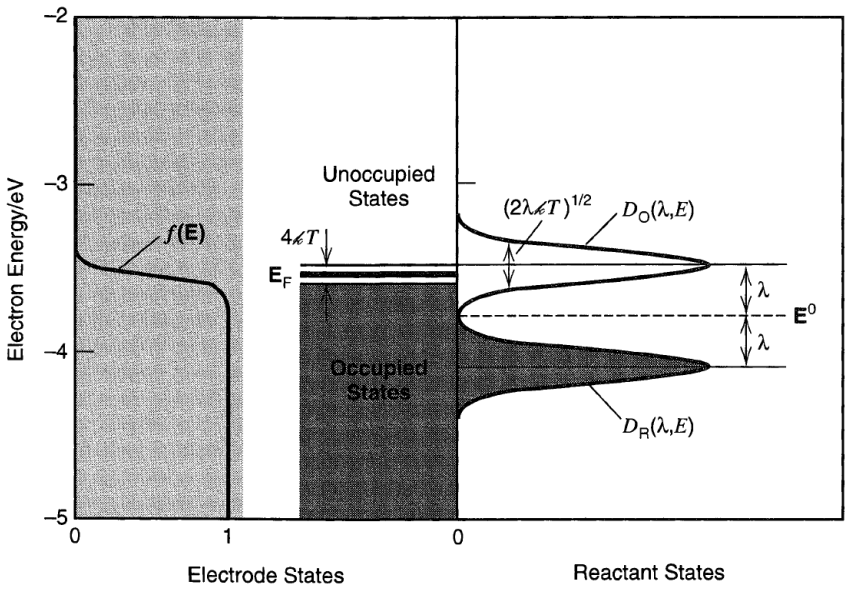

Figure 1: Representation of the electronic energy states on the electrode and the reactant. The energy of electrons is on the vertical axis in electron volts. In the metal electrode there is a zone with the width of $4k_BT$ centered on the Fermi level where the Fermi function $f(\mathbb{E})$ transitions from 1 to 0. The Fermi function describes at what probability a specific state of energy $\mathbb{E}$ is occupied by an electron. In the solution the energy levels of the oxidant and the reductant are gaussian state density distributions and depending on how they are positioned in relation to the Fermi level oxidation or reduction reactions can be blocked. Here the filled electronic energy states of the metal electrode are overlapping with the empty O states the reduction reaction can occur. Oxidation on the other hand is blocked as all filled R states overlap only with other filled states of the electrode. By applying a potential to the electrode the location of Fermi level can be changed and then the reaction direction could be reversed. Figure by Bard and Faulkner [2].

This can be discussed further by using copper chloride salt ($CuCl_2$) as an example. The electrolyte solution is formed by dissolution of $CuCl_2$ in water, which leads to the molecule breaking down to one Cu^{2+} and two Cl^- ions. When DC

voltage is applied, a current starts flowing through the cell resulting in positively charged species migrating to the negative electrode while the negatively charged species travel to the positive electrode. At the positive electrode the negatively charged chlorine ions are oxidized resulting in them losing their electron and forming chlorine gas.

$$2Cl^- \rightarrow Cl_2 + 2e^-$$

At the same on the negative electrode the copper ions are plated out as metallic copper.

$$Cu^{2+} + 2e^- \rightarrow Cu^0$$

This reaction is also an example of chemically irreversible reaction meaning that the reverse reaction is not possible in the electrochemical cell by reversing the potentials, which is in this case characterized by formation of gas which leaves the system. Other causes for a reaction to be irreversible are different reactions occurring or new side products being created when the current is reversed [3].

Cynthia Zoski [3] gives the following reaction as an example of a chemically reversible reaction as the reactions don't produce other reactions or side products when the current is reversed:

$$Sn^{2+} + 2Fe^{3+} \rightleftharpoons 2Fe^{2+} + Sn^{4+}.$$

Reactions in an electrochemical cell can also be distinguished by whether they happen spontaneously or if a potential needs to be applied in order for the reaction to occur. Cells where a reaction occurs spontaneously once the electrodes are connected are known as galvanic cells. Prime example of a galvanic cell is a battery where the reaction begins the moment it's terminals are connected via a circuit.

Cells that need a potential applied to them in order to produce a reaction are known as electrolytic cells. Electrolytic cells are very common in industry, e.g. in the production of metallic aluminum from alumina, and in day to day life, as rechargeable batteries (e.g. Cu and Zn) function as electrolytic cells when they are recharged [3].

2 Electrochemical cell

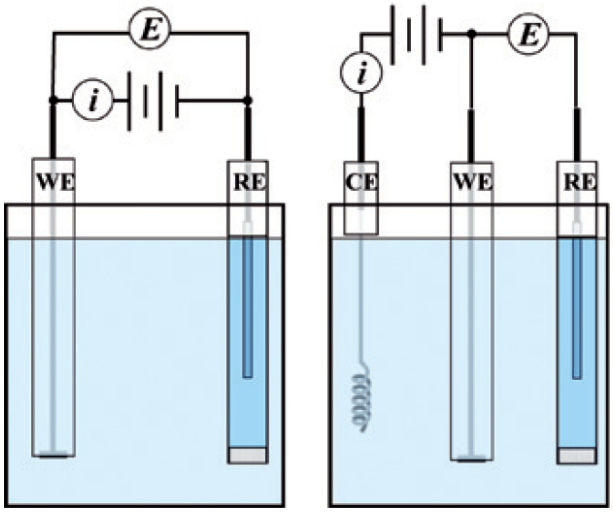

Figure 2: Schematics of a two-electrode electrochemical cell and a three-electrode chemical cell. In three-electrode system a separate reference electrode is added to serve as the potential against which all other potentials in the system are measured. Image by Zoski [3].

Each electrochemical reaction is composed of two half-reactions, reduction and oxidation, commonly termed as redox reaction, where

$$\mathrm{Ox}_1 + ne^- \rightarrow \mathrm{Red}_1 \qquad \text{and} \tag{1}$$

$$\mathrm{Red}_2 \rightarrow \mathrm{Ox}_2 + ne^-. \tag{2}$$

Reaction (1) is the oxidation reaction where one electrochemical species gives off one or more electrons and reduces. Reaction (2) is this reaction's counterpart where the species receives electrons and becomes oxidized. In total this reaction can be written as

$$\mathrm{Ox}_1 + \mathrm{Red}_1 \rightarrow \mathrm{Red}_2 + \mathrm{Ox}_2. \tag{3}$$

Each reaction occurs spontaneously in one direction, the one where the change in Gibbs free energy ΔG is negative.

$$\Delta G = \Delta G^0 + RT\ln\frac{a_{\mathrm{Red}}a_{\mathrm{H^+}}}{a_{\mathrm{Ox}}a_{\mathrm{H_2}}}, \tag{4}$$

where a_{Red} and a_{Ox} are the activities of the reductant and oxdidant, respectively, and $a_{\mathrm{H_2}}$ and $a_{\mathrm{H^+}}$ are activities of hydrogen molecules and hydrogen ions, respectively, and are usually assumed to be unity [2].

Electrochemical redox reactions occur in electrochemical cells, which are generally composed of three main components. First, electrolyte with the chemical species of interest must be prepared, and while solid media are sometimes used, liquid media are much more common and they are usually water-based solutions. Secondly, electrodes, which provide the boundaries where the electrochemical reactions occur, must be inserted into the electrolyte.The electrodes are connected by the final component, the external circuit, which allows the transfer of electrons from one electrode to the other. The current and potential difference between the electrodes can be measured or controlled. Herein lies what separates electrochemistry from normal chemistry. In both the reactions are controlled by temperature, pressure and concentration but in electrochemistry an additional parameter, potential, is added. By controlling the potential the balance of the reaction can be controlled or the direction of the reaction can be reversed.

2.1 Electrodes

While only two electrodes are necessary for an electrochemical reaction, most reactions are done in a cell using a three-electrode system where a third electrode is added. These are usually named working electrode, counter electrode, also known as auxiliary electrode, and reference electrode.

2.1.1 Working electrode

Usually only one of the half-reactions happening in the electrochemical cell is of interest, e.g. electrocrystallization on the electrode surface. The electrode were the reaction of interest takes place is known as a working electrode. The potential of this electrode is measured against a reference electrode. The current going through the working electrode can be manipulated by changing its potential [1, 4, 5].

A good working electrode has to have certain characteristics such as: stable and reproducible chemical, structural and electrical properties, good electrical conductivity, stability, both chemical and electrochemical, in the system in question and finally a quick electron transfer rate in many different systems [3]. Most of the previous characteristics are properties of the material itself but there are factors that can wildly affect the electron transfer on the electrode surface. Zoski [3, p. 111] lists the following factors: "(i) type of electrode material, (ii) surface cleanliness, (iii) surface microstructure, (iv) surface chemistry, and (v) electronic properties (e.g. charge carrier mobility and concentration[...]." It should be noted that the depending on the type of the reaction, whether it is a inner sphere reaction, where the reaction occurs at the electrode surface, or an outer sphere reaction, where the reaction occurs away from the electrode, the type of the electrode material may or may not affect the reaction. [2] Surface microstructure and crystal orientation e.g. can directly affect the growth of resulting layers in electrodeposition of metals and it's possible to find electrodes with different crystal orientations or porosity.

Common materials for electrodes are inert metals such as platinum, different forms of carbon such as graphite or glassy carbon, or semiconductors e.g. indium tin oxide [1]. Each of these materials comes with their own pros and cons and different procedures when it comes to handling them. All electrodes share a common factor, that is they have to be cleaned and possibly pretreated before being used in actual measurements. Air is one of the most common electrode contaminants,

especially with carbon-based electrodes, as particles in the air can adsorb on to the electrode surface changing the electrode kinetics. In addition, oxygen in the air can react with the pure carbon on the electrode surface changing its chemical properties and microstructure. Thus electrodes must be cleaned and otherwise pretreated to get rid of contaminants from the environment and possible residue from previous experiments with the electrode [3].

Glassy carbon, also known as vitreous carbon, is one of the most used working electrodes. Glassy carbon doesn't have a repeating crystal structure but it is made out of interwoven sheets of graphite and thus is much harder than other forms of graphite [6]. The surface of glassy carbon electrodes is gradually contaminated with exposure to air and they have to be polished and activated before being used in experiments. Mechanical polishing with alumina (Al_2O_3) is a common way to remove these contaminants. A slurry of alumina suspended in distilled water with grain sized ranging form 1 μm to 0,05 μm is used to polish the electrode against polishing pads in a figure-eight motion to remove the particles on the electrode surface [3, 7]. Polishing also removes some of carbon and thus leaving some dangling bonds where atmospheric oxygen atoms can attach themselves. This layer of can be removed by conditioning the electrode with polarizing it with a gradual potential scan [3]. The electrodes should be used immediately after polishing in order to avoid contamination by air.

2.1.2 Counter electrode

A counter electrode is the electrode that is connected to the working electrode via an external circuit. Its function is to create an electric field into the electrolyte solution along with the working electrode allowing for an electric current between the two electrodes. Requirement for the counter electrode is that it doesn't limit the amount of current and thus the reaction rate. This can be achieved by making the surface

area of counter electrode much larger than that of the working electrode. Counter electrodes should be inert and not produce any undesired reaction products by electrolysis as such species could reach the working electrode and cause interfering reactions there. Counter electrodes might be placed in a separate compartment away from the working electrode with some kind of separator, such as a sintered glass membrane, between them to avoid this, although in practice this isn't usually a problem due to the slow diffusion rate of the produced substances [1, 4, 5].

2.1.3 Reference electrode

While reference electrodes are not necessary for the reactions in the cell, they are extremely widely used for measuring the potential of the working electrode. It's not possible to have an absolute measure of potential as only potential differences are measurable. Thus a standard reference point is defined using the Standard Hydrogen Electrode (SHE) where the controlling redox process is

$$2H^+ + 2e^- \rightleftharpoons H_2$$

and the standard potential of this reaction is assigned as 0.0000 volts (V) at all temperatures. [3] According to Hamann *et. al.* [5] the Standard Hydrogen Electrode "consists of a platinised platinum sheet immersed in aqueous solution of unit activity of H^+(aq) in contact with hydrogen gas at a pressure of one atmosphere." The potential of all other reference electrodes is measured against the potential of the SHE.

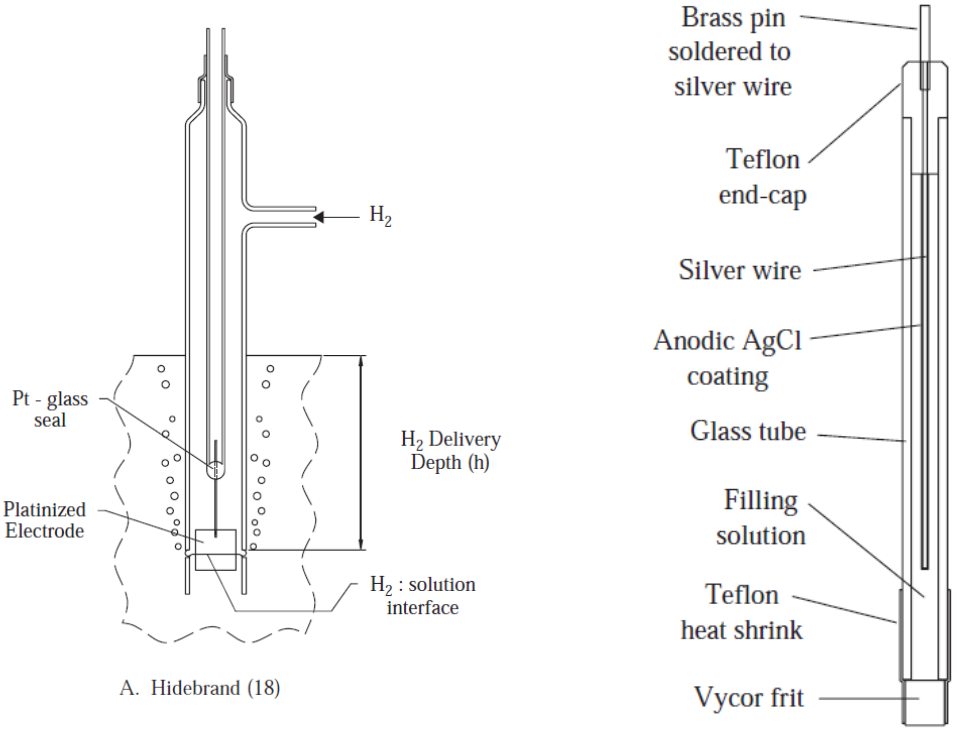

Figure 3: a) Standard Hydrogen Electrode, b) Ag-AgCl reference electrode. Images by Cynthia Zoski [3].

The Standard Hydrogen Electrode is not the easiest reference electrode to use as it requires bubbling gasses and many of its parameters must be quite exact. There are many other reference electrodes that are easier to use, one of which have also been used in the experiments performed in this study, that is the silver–silver-chloride electrode where the controlling redox process is

$$\mathrm{AgCl} + \mathrm{e}^- \rightleftharpoons \mathrm{Ag} + \mathrm{Cl}^-.$$

The standard potential of this reaction is 0,222 V versus the SHE at 25 °C. As the activities of AgCl and Ag are 1, due to them being solids, the overall potential depends solely on the concentration of chlorine ions in the solution according to the Nernst equation, which is presented in the next chapter. Ag/AgCl reference

electrodes are used because of their simple design, inexpensive materials, nontoxic components, and they can be manufactured with normal electrochemistry equipment easily [3].

2.2 Electrolyte solution

Electrochemical reactions occur at the boundary of an electrode and an electrolyte. Electrolyte is the medium that is composed of a solvent and dissolved ions. The dissolved ions carry current flow through the electrolyte solution when an electric field is applied. The dissolved ions then flow trying to maintain charge balance in the solution between the working and counter electrodes. How well an electrolyte solution supports current flow is measured by conductivity, which is the reciprocal of resistivity, and it's units are $\Omega^{-1}\text{cm}^{-1}$. Conductivity depends on many different factors but generally two main factors can be identified [3].

First the concentration of charge carriers e.g. dissolved ions. If the concentration of charge carriers is low then the conductivity is small meaning that the flow of current through the electrolyte is inhibited. [3] This is solved by adding a supporting electrolyte, which has much higher concentrations than the electrolyte used in the reaction of interest, that makes sure the current can flow freely [1]. This is covered in more detail in Section 3.1.

The second factor affecting the ionic conductivity is how well the ions move in the applied electric field. This is described by ion mobility u_i of a specific ion i which is the velocity of the ion in an electric field. Ion mobility, assuming spherical shape, depends on the charge of the ion, its radius and the viscosity of the fluid. The ions have a harder time moving in viscous fluid and the larger their radius is more they will collide with other particles. Both of these effects reduce the mobility of ions. [3]

The actual current flow depends primarily on the conductivity of the solution

and the geometry of the electrodes. Shape and size both have an effect on the electric resistance of the solution but generally the resistance increases as the size of the electrode is decreased. The product of the solution resistance and the current in the cell is known as ohmic loss. As mentioned earlier ohmic losses affect the measured potentials if the potential is measured by the same electrode by which the current is flowing through. This can be mostly fixed by having a solution with high conductivity and by using a reference electrode [1, 3].

Secondarily the current distribution is affected by the kinetics of the occurring reactions and the reaction itself. Tertiary effect comes from the local changes in density of the supporting electrolyte which leads to changes in the velocities of the electroactive species. This effect is not reduced even with larger concentrations of supporting electrolyte [8].

2.3 Capacitance and the double layer

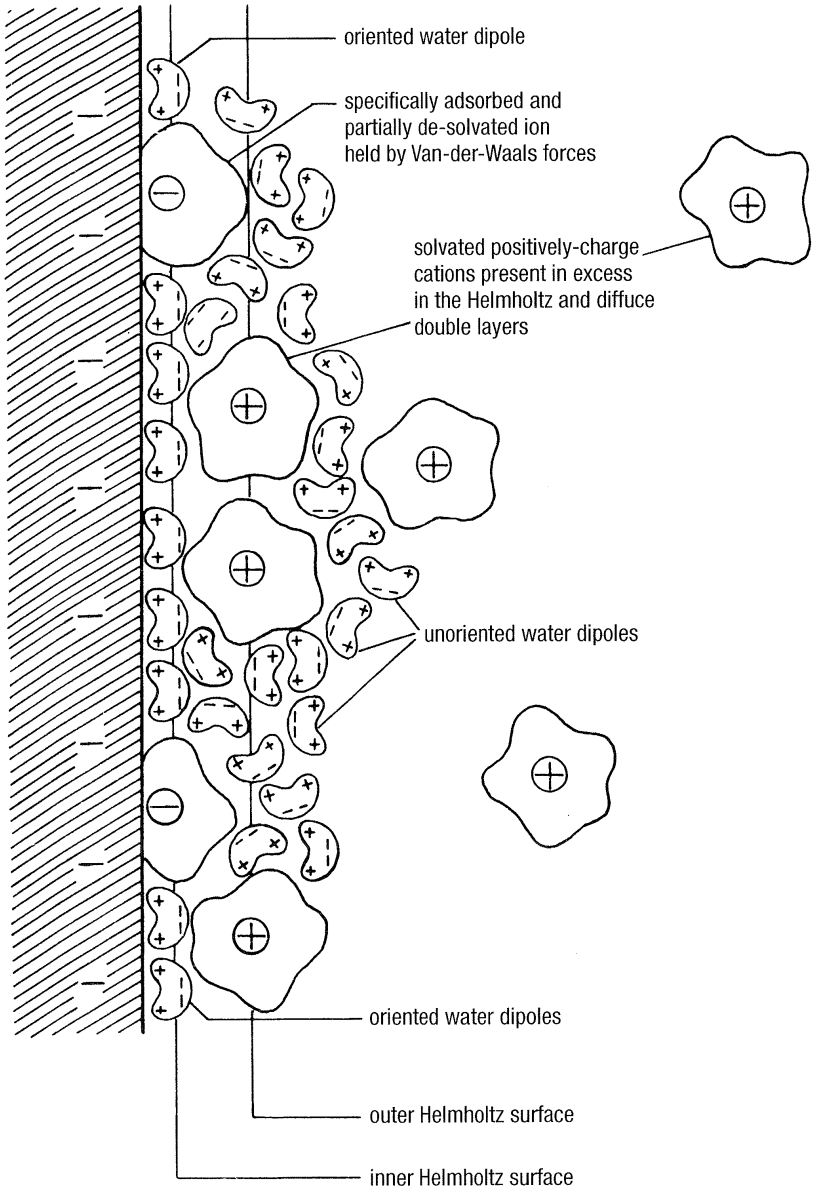

Figure 4: Schematic of the double layer and its molecular structure for a negative electrode surface. It resembles a parallel plate capacitor with ions and oriented water dipoles as the plates of the capacitor. Image by Hamann, Hamnett and Vielstrich [5].

Electrochemical reactions occur at the boundary between electrode and electrolyte solution. The volume close to boundary behaves differently from the bulk electrolyte where charge neutrality is conserved. Near the electrode surface charged species such as ions can accumulate or dipolar molecules such as water molecules can orient themselves in a way that creates an excess of charge on the electrolyte layer near the boundary. The excess charge creates an electric field. The area of the excess charge is known as the double layer [1].

The double layer can be thought of consisting of three layers. The one closest to the electrode surface is known as the inner Helmholtz layer where ions are *specifically adsorbed* to the surface. [4] In specific adsorption the chemical species in question is affected by interactions between the species and the surface beyond the Coulombic interaction such as by van der Waals interactions [1, 5]. Negatively charged particles, solvent molecules or other non-charged molecules can be specifically adsorbed whereas positively charged particles can't usually be specifically adsorberd. [1] As can be seen in Figure 4 water molecules are highly polar and they can orient themselves to form a charged layer.

The outer Helmholtz layer is created by the closest solvated ions to the inner Helmholtz layer. Ions can't reach the electrode surface due to the inner layer being in their way and the ions only interact with the electrode surface by long range electrostatic forces. This means that the interaction between ions at the outer Helmholtz layer and the electrode are mostly independent of their chemical properties and they are considered *nonspecifically adsorbed* [1, 4, 5].

The region between the outer Helmholtz layer and the bulk of the electrolyte is known as diffuse layer, although the borders of this region are nonspecific. In the diffuse layer the chemical species are loosely ordered by thermal movement and by the strength of the electrostatic forces with them being more disordered as the species gets farther from the electrode surface. The thickness of the diffuse layer is

dependent on the concentration of the chemical species [1, 4].

3 Theoretical background

There are many different factors that affect the reactions occurring on the electrode surfaces. In the following examinations only simple reduction and oxidation processes are considered, where

$$\mathrm{O} + ne^- \rightleftharpoons \mathrm{R}. \tag{5}$$

The simplest way to consider the potential of an electrochemical cell E at equilibrium is by using the Nernst equation which is only valid a reversible reactions and only in systems with fast kinetics. [3, 4]

$$E = E^{0\prime} + \frac{RT}{nF}\ln\frac{C^*_{\mathrm{ox}}}{C^*_{\mathrm{red}}}, \tag{6}$$

where $E^{0\prime}$ is the formal potential, R is the gas constant (8,314462 J K^{-1} mol^{-1})[1], T [K] is temperature, n is the number of electrons exchanged between oxidant and reductant, F is the Faraday constant (96485 C·mol^{-1})[1], and C^*_{ox} and C^*_{red} are the bulk concentrations of oxidant and reductant, respectively [3].

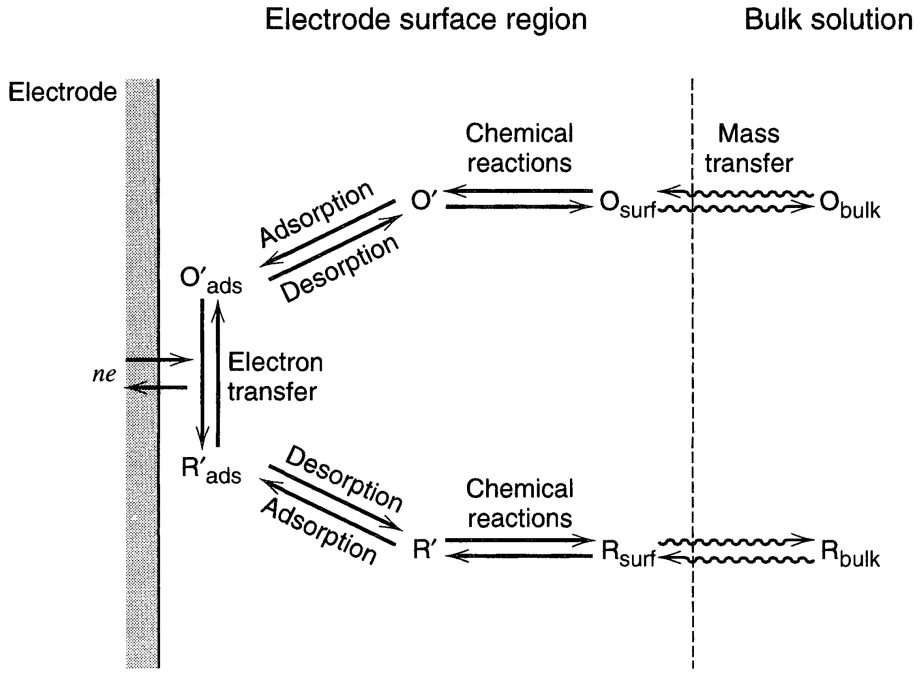

Figure 5: The reaction steps for a general electrode reaction. Image by Bard and Faulkner [4].

Bard and Faulkner [4] say that in general the overall electrode reaction rate i.e. current is governed by four different processes:

1. Mass transfer of chemical species to the electrode surface.
2. Transfer of electrons at the electrode surface.
3. Possible chemical reactions that occur at the electrode surface either before or after the electron transfer.
4. Other reactions, such as adsorption or electrodeposition, happening on the electrode surface.

The current in an electrochemical cell is limited by the slowest of the reaction steps that participate in the overall reaction. While many of the reaction steps might be fast, even one slow reaction step inhibits the total reaction rate. These limiting reaction steps are called rate-determining steps.

3.1 Mass transfer

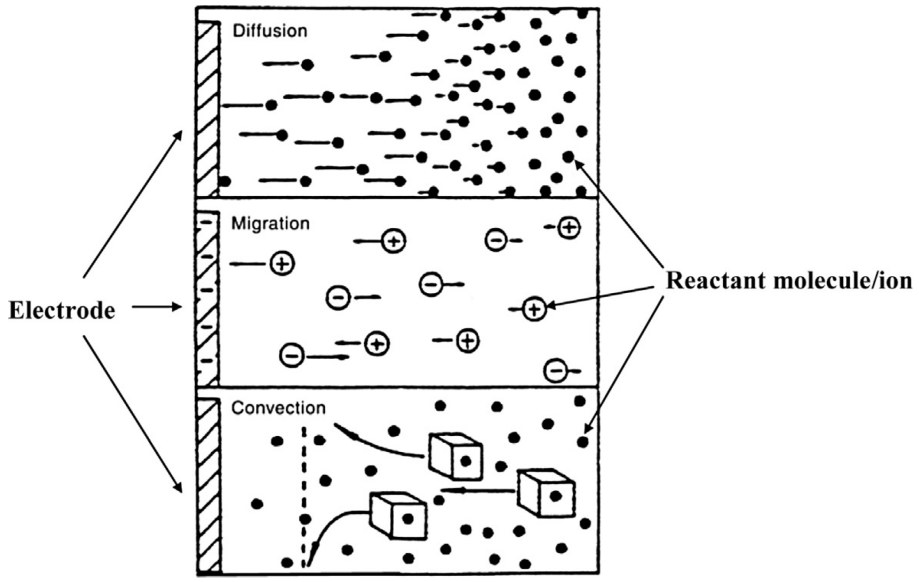

Figure 6: Three different types of mass transport. Diffusion is Brownian motion where concentration differences try to even out. Migration is the movement of ions due to an electric field between working and counter electrodes. Convection is movement of fluid element by movement of the solution itself. Image by Weiwei Cai et. al. [9].

It is important to consider the processes by which the mass is transferred from anode to cathode and vice versa. Mass transfer is caused by differences in the electrochemical potential

$$\bar{\mu} = \mu^0 + RT \ \mathrm{ln}a + zF\phi, \tag{7}$$

where μ^0 is the standard chemical potential, a is the activity, z is the charge and ϕ is the local electrostatic potential [4]. The mass flux $\mathbf{J}_j$ of species j is proportional to the gradient of the electrochemical potential

$$\mathbf{J}_j = -L\nabla\bar{\mu}, \tag{8}$$

where L is a so called phenomenological factor [1]. This can be written as the steady-state *Nernst–Planck equation* by adding a term that takes the possible convection, i.e. flow of the electrolyte solution

$$\mathbf{J}_j = -D_j\nabla C_j - \frac{z_j F}{RT} D_j C_j \nabla\phi + C_j\mathbf{v}, \tag{9}$$

where D_j is the diffusion coefficient, C_j is the concentration, z_j is the charge of the species j, ϕ is the electric field and finally $\mathbf{v}$ is the velocity of a volume element within the solution.

The first term is the diffusion term. It describes that concentration differences try to even out due to Brownian motion following the gradient of the concentration. The second term is the migration term, which expresses the movement of charged particles under the influence of an electric field. The last term as described above takes into account convection within the liquid e.g. when it's stirred [4].

In the bulk of the solution it's assumed that there are no concentration differences so there are only migration and convection. If the solution is not stirred then only the migration term remains. Thus in the bulk of the solution the mass transfer is mostly driven by the gradient of the electric field. [1] However, usually the region of interest is near the electrodes where the situation is different. Due to the viscosity the fluid the velocity of the fluid on the surface of the electrode is zero[10]. This forms a thin coating that doesn't mix, so the effect of the migration is reduced and diffusion plays the key part in the mass transport near the electrode surface[1]. To further reduce the effect of migration near the electrode surface a supporting electrolyte with much higher concentration is added to the solution. The supporting electrolyte consists of non-electroactive ions that don't effect the reaction of interest near the electrode.

Its main function is to function as the charge carrier in the solution. Thus the approximation can be made that the ions of the reactive species don't carry any charge and their mass transfer occurs only by diffusion near the electrode surface. [1, 4] In practice the solution should have about two orders of magnitude more of the supporting electrolyte than the reactive electrolyte species so that the effects of migration on the mass transfer become minuscule [4, 5].

Equation (4), however, only describes a steady-state mass transfer. To consider the case where the concentration changes as a function of time and place the nonsteady-state function must be acquired by taking the divergence of Nernst–Planck equation

$$\begin{aligned} \frac{\partial c_j}{\partial t} &= -\nabla \cdot \mathbf{J}_j \\ &= D_j \nabla^2 C_j + \frac{z_j F}{RT} D_j \left(\nabla C_j \cdot \nabla \phi + C_j \nabla^2 \phi \right) - \left(C_j \nabla \cdot \mathbf{v} + \mathbf{v} \cdot \nabla C_j \right) \end{aligned} \tag{10}$$

This assumes that diffusion coefficient is not dependent on concentration[1]. In electroneutral case $\nabla^2 \phi = 0$ and if the solution is assumed to be incompressible, that is it has no sources or sinks, then $\nabla \cdot \mathbf{v} = 0$, and a simplified expression can be acquired

$$\frac{\partial C_j}{\partial t} = D_j \nabla^2 C_j + \frac{z_j F}{RT} D_j \nabla C_j \cdot \nabla \phi - \mathbf{v} \cdot \nabla C_j. \tag{11}$$

By adding a supporting electrolyte to the solution the migration of the particles of interest can be approximated as $\nabla \phi \approx 0$ because the supporting electrolyte carries most of the current in the system. Convection term $\mathbf{v} \cdot \nabla C_j$ can be removed if no forced movement, such as stirring, is applied to the solution [1] and then the equation (6) can be reduced to the *Fick's second law*

$$\frac{\partial C_j}{\partial t} = D_j \nabla^2 C_j. \tag{12}$$

However there are actually two different processes which participate into the reaction. First is the diffusion of the reactant which is described by the Nernst–Planck equation and the second is the electron transfer reaction at the electrode boundary. Diffusion alone is not able to explain whether or not a reaction occurs at an electrode or what the reaction rate is. Those questions are answered by electrode *kinetics*. [9, 11]

3.2 Kinetics

In an electrochemical reaction the reactants, oxidant and reductant, have to reach the electrode surface in order for the electron transfer to happen. The reactants reach the electrode surface by diffusion as discussed previously, but the reaction itself doesn't depend on diffusion. Taking a simple example reaction

$$\mathrm{O} + ne^- \underset{k_{\mathrm{red}}}{\overset{k_{\mathrm{ox}}}{\rightleftharpoons}} \mathrm{R} \tag{13}$$

where O is the oxidized species, R is the reduced species, n is the electron transfer number, which is usually 1, and finally k_{ox} and k_{red} represent the oxidation and reduction reaction rate constants, respectively.[9] The reaction rates are often expressed by Arrhenius formula by writing

$$k_{\mathrm{ox}} = A_{\mathrm{ox}} \exp\left(\frac{-\Delta G_{\mathrm{ox}}}{RT}\right) \tag{14}$$

$$k_{\mathrm{red}} = A_{\mathrm{red}} \exp\left(\frac{-\Delta G_{\mathrm{red}}}{RT}\right), \tag{15}$$

where A_{ox} and A_{red} are the Arrhenius constants representing the reaction rates at unlimited temperature (T) and ΔG_{ox} and ΔG_{ox} are Gibbs free energies, for oxidation and reduction reactions, respectively. The Gibbs free energy for oxidation ΔG_{ox} can be thought of as the energy barrier that the oxidized species must cross to reduce and similarly ΔG_{ox} is the energy barrier that the reduced species must cross in order to become a oxidized as presented in Figure 7. [4, 9]

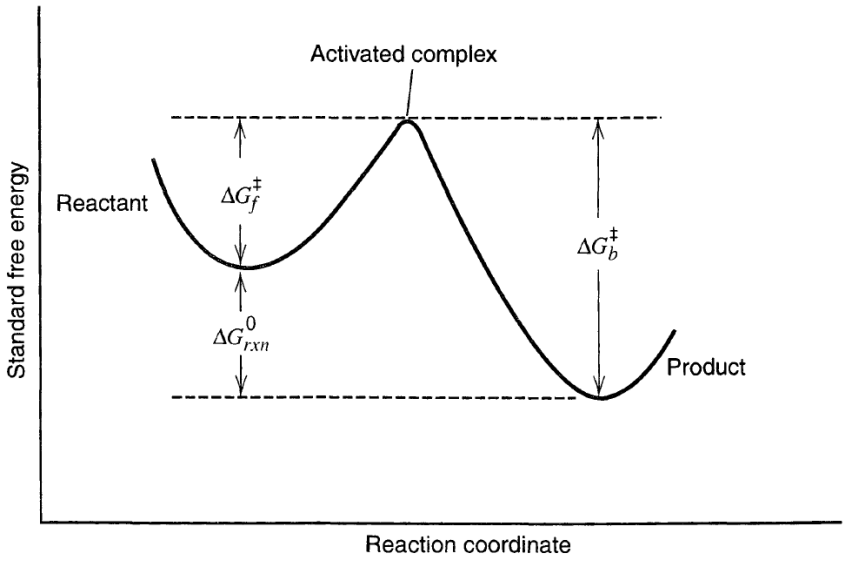

Figure 7: Changes in Gibbs free energies during a reaction. A barrier of standard free energy must be overcome in order for a reactant to become a product. Image by Bard and Faulkner [4].

Reaction rates v_{ox} and v_{red} can be written using the reaction rate constants oxidation and reduction as

$$v_{\text{ox}} = k_{\text{ox}} C_{\text{ox}}(0,t) \tag{16}$$

$$v_{\text{red}} = k_{\text{red}} C_{\text{ox}}(0,t), \tag{17}$$

where $C_{\text{ox}}(0,t)$ and $C_{\text{ox}}(0,t)$ are the concentrations of oxidized and reduced species at the electrode surface, respectively and t is time. Within the bulk solutions the corresponding concentrations are written as $C_{\text{ox}}(x,t)$ and $C_{\text{red}}(x,t)$ where x is the distance from the electrode surface. When the reaction reaches equilibrium the reaction rates of oxidation and reduction are equal [9].

$$k_{\text{ox}} C_{\text{ox}}(0,t) = k_{\text{red}} C_{\text{red}}(0,t) \tag{18}$$

According to Weiwei Cai *et. al.* [9] equations (16), (17) and (18) can be combined along with changing the oxidation and reduction reaction rates into current densities, currents for oxidation and reduction reaction can be obtained

$$j_{\text{ox}} = nFk_{\text{ox}}C_{\text{ox}}(0,t) \tag{19}$$

$$j_{\text{red}} = nFk_{\text{red}}C_{\text{red}}(0,t). \tag{20}$$

Oxidation and reduction current densities, j_{ox} and j_{red}, can also be written as anodic and cathodic current densities, j_a and j_c, respectively [11]. In the case of electrochemical nucleation Equation (20) can also be written as

$$j_{\text{red}} = nFk_{\text{red}}a_{\text{red}} \tag{21}$$

where a_{red} is the activity coefficient of reduction, which is equal to unity [2].

In Figure 8 the electrode potential is changed from E^0 to E which causes the Gibbs free energy of oxidation to change from ΔG^0_{ox} to ΔG_{ox} and similarly for reduction ΔG^0_{red} changes to ΔG_{red}. In normal cases changing the potential of the electrode affects only the energy of its electrons which results in total change of $\alpha nF(E - E^0)$, where α is so called electron-transfer coefficient that can have values between zero and one. Its purpose can be seen from Figure 8, where it is used to take into account the fact that not all of the potential change $F(E - E^0)$ goes towards crossing the potential boundary [4, 9].

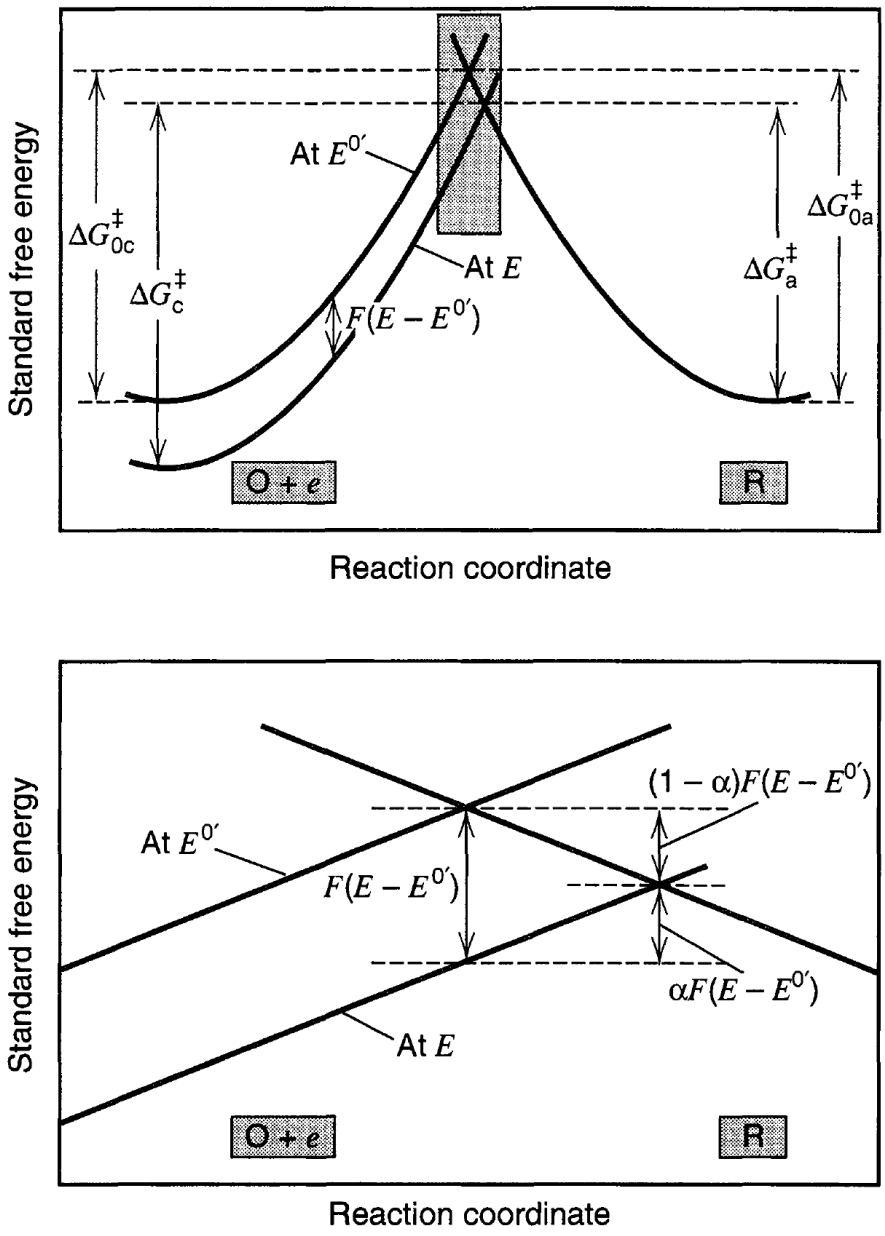

Figure 8: Changing the potentials from E to E_0 affects the standard free energies of activation for both oxidation and reduction. From the lower image, which represents the boxed area in the upper image, the electron-transfer coefficient is introduced. Image by Bard and Faulkner [4].

Using the electron-transfer coefficient and the change in electrode energies $\alpha nF(E-E^0)$ the net current density can be written as

$$j = j_{\text{ox}} - j_{\text{red}} = nF\left[k^0_{\text{ox}}\ C_{\text{ox}}(0,t)\ \exp\left(-\frac{(1-\alpha)nF(E-E^0)}{RT}\right)\right.$$
$$\left. - k^0_{\text{red}}\ C_{\text{red}}(0,t)\ \exp\left(-\frac{\alpha nF(E-E^0)}{RT}\right)\right] \tag{22}$$

where k^0_{ox} and k^0_{red} are the reaction rate constants at the potential E_0. According to Weiwei Cai *et.al.* [9] at standard conditions (25 °C, 1 atm and $C_{\text{ox}}(0,t) = C_{\text{red}}(0,t) = 1.0$ mol dm^{-3}) and based on Equation (13) k_{ox} and k_{red} are equal

$$k^0_{\text{ox}} = k^0_{\text{red}} = k^0 \tag{23}$$

where k^0 is known as the standard rate constant. Using it Equation (16) can be written as

$$j = j_{\text{ox}} - j_{\text{red}} = nFk^0\left[C_{\text{ox}}(0,t)\ \exp\left(-\frac{(1-\alpha)nF(E-E^0)}{RT}\right)\right.$$
$$\left. C_{\text{red}}(0,t)\ \exp\left(-\frac{\alpha nF(E-E^0)}{RT}\right)\right]. \tag{24}$$

Equations (22) and (24) are known as Butler-Volmer equations in honor two trailblazers of this field. This equation is among the most important equations describing surface reactions in electrochemical cells. [4, 9] According to the equation the current is exponentially proportional to the magnitude of the potential step $E - E_0$.

3.3 Nucleation

At the very early stages of electrochemical deposition the process might not be diffusion limited, as is the usual assumption, but the deposition becomes limited by the limited number of initial surface nucleation sites where particles can attach and by the rate at which new sites are created. The initial nucleation sites are

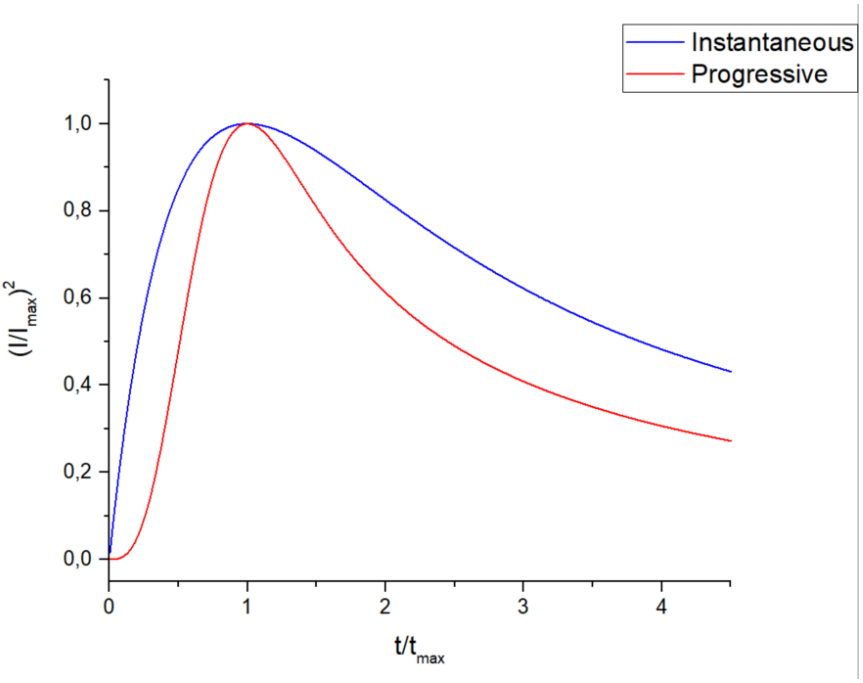

Figure 9: Dimensionless I/I_{max} plot for both instantaneous and progressive nucleation mechanisms [12].

composed of different kinds of surface defects which are also known as active sites. [5] There are in general two types of nucleation depending on the behavior of active sites. If (nearly) all of the active sites are created at the initial step of applied overpotential required to initiate the reaction, then the nucleation process is known as *instantaneous nucleation* whereas if the nucleation sites are created over time, then the process is known as *progressive nucleation*. In truth any real electrochemical deposition process exhibits both instantaneous and progressive nucleation at the same time but at varying degrees. [12] These types of nucleation are described by Benjamin Scharifker and Graham Hills [12] in their seminal paper where they derived dimensionless formulas that can be used to determine the type of nucleation based on chronoamperometric measurements:

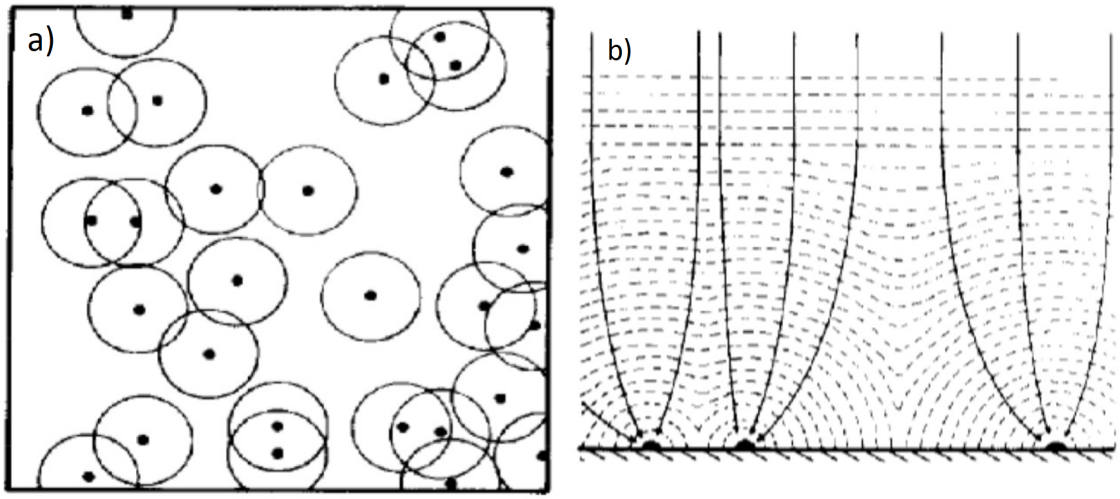

Figure 10: a) Planar view of the hemispherical nuclei diffusion zones which start growing from their initial locations along with the nuclei themselves leading to overlapping zones where no new nuclei can form. b) Each nuclei distort the local electric field growth of which leads to eventual overlapping of the diffusion zones. Both images by Scharifker and Hills [12].

$$\frac{I^2}{I_{max}^2} = \frac{1,9542}{t/t_{max}} \left\{1 - \exp\left[-1,2564(t/t_{max})\right]\right\}^2 \qquad \text{instantaneous nucleation, and} \tag{25}$$

$$\frac{I^2}{I_{max}^2} = \frac{1,2254}{t/t_{max}} \left\{1 - \exp\left[-2,3367(t/t_{max})^2\right]\right\}^2 \qquad \text{for progressive nucleation,} \tag{26}$$

where I_{max} and t_{max} are the maximum value of current and the time after the potential step at which the maximum current occurred. These functions are plotted in Figure 9.

The derivation of these formulas is beyond the scope of this thesis but the intuition behind the process will be explained in more detail. The basic assumption is that the growth of a nucleus is described by spherical diffusion and each nucleus has a growing hemispherical diffusion zone. This description is however valid for only

individual nuclei, which might be the case for experiments with micro- and nano-electrodes. In reality in most systems there are many nuclei that can't be assumed to grow independent of each other as each nucleus develops a diffusion zone around themselves that where the dissolved electroactive species deposits to the growing nucleus instead of creating a new active site by reaching the electrode surface, this is presented in Figure 10a. This exclusion zone is formed due to the growing nucleus deforming the local electric field as presented in Figure 10b. To this, Scharifker and Hills do note that the presence of a supporting electrolyte greatly reduces the deformation of the electric field adding that still the concentration of particles near a nucleus under mass-transfer control is lower than in the bulk and thus reducing the probability of creation of a new nucleus near an already growing nucleus. This exclusion zone grows with the nuclei and starts to overlap with the diffusion zones of other growing nuclei. Due to this most of the growth happens at sites that are not within another exclusion zone. Eventually the entire surface is covered by the nuclei leading to a surface, which has effectively planar diffusion zone [12].

With this in mind, instantaneous nucleation sees the formation of nearly all nuclei immediately after applying the potential step. In this case all of the nuclei can be thought to be the same age and as such grow at the same rate. In progressive nucleation on the other hand not all nuclei for immediately, but they are formed gradually over some time after the potentiostatic step. [12, 13] Thus the type of nucleation can be determined by seeing which function (19) for instantaneous or (20) for progressive nucleation fits the potentiostatic data better. This has been done for the experimental data in section 6.

There is also another, more precise model developed by Heerman and Tarallo [14] which combined two earlier approaches by Scharifker–Mostany and Sluyter–Rehbach, from which quantitative values for nucleation constant per active site A, number density of active sites of the surface N_0 and diffusion coefficient D can be

obtained by fitting them to the following expression of current density j in units of A cm^{-2}:

$$j(t) = zFDc\frac{1}{(\pi Dt)^{1/2}}\frac{\Phi}{\Theta}\left(1 - \exp\left[-\alpha N_{\mathrm{o}}(\pi Dt)^{1/2}t^{1/2}\Theta\right]\right), \tag{27}$$

where

$$\Phi = 1 - \frac{\exp(-At)}{(At)^{1/2}}\int_0^{(At)^{1/2}} \exp\left(\lambda^2\right) d\lambda \tag{28}$$

$$\Theta = 1 - \frac{\left(1 - e^{-At}\right)}{At}, \tag{29}$$

and where z is the number of transferred electrons, F is the Faraday constant (96485 C/mol), c is the concentration of the metal ions in the bulk solution, $\alpha = 2\pi(2MDc/\rho)^{1/2}$, where ρ is the density of the deposited metal, and M is the molar mass of the deposit. [13, 15] According to D. Lomax *et. al.* [15] the term Φ is related to Dawson integral and it can be approximated numerically with Equation 24. This models how the concentration of precursor ions depletes over time near the electrode surface.

$$\begin{aligned}\Phi &= 1 - \frac{\exp(-At)}{(At)^{1/2}}\int_0^{(At)^{1/2}} \exp\left(\lambda^2\right) d\lambda \\ &= 1 - \left[\frac{e^{-At}}{(at)^{1/2}}\left(\frac{0,05131 + 1,47910725(At)}{1 - 1,2068142(At)^{1/2} + 1,118572(At)}\right)\right]\end{aligned} \tag{30}$$

Parameters A, N_0 and D can be obtained by fitting to the experimental chronoamperometric data. This is done for the experimental values in section 6.

4 Electrochemical methods

There are many types of measurements that can be performed to evaluate different processes occurring at the electrode surfaces. In this study two are in the focus, chronoamperometry and cyclic voltammetry. According to Zoski [3] when considering electrochemical experiments their mass transfer should always be under diffusion-control and that there are a few ways to achieve this:

- Having a large enough concentration of supporting electrolyte so that they carry the current in the electrolyte instead of the chemical species of interest.
- Eliminating convection within the solution, including natural convection induced by experiments that are longer than 30 seconds, OR
- by introducing forced convection and using a rotating electrode to limit the thickness of the diffusion layer.

4.1 Chronoamperometry

Let us consider the reduction reaction

$$\mathrm{Ox} + ne^- \rightarrow \mathrm{Red} \tag{31}$$

The simplest way to acquire knowledge of this reaction is chronoamperometry where the behaviour of current is measured against time when the potential of the working electrode is changed by a potential step. Potential is changed from the initial potential E_i to the final potential E_f in an instant. E_f should be selected as such that the reaction interest, in this case reduction, happens at that potential. E_f is selected so that the concentration of the reactant goes zero at the electrode surface i.e. all of the oxidant that approaches the surface gets reduced [3].

The current transient for an electrode is described by the *Cottrell equation*,

$$i(t) = \frac{nFAD_{\text{ox}}^{1/2}C_{\text{ox}}^{*}}{\pi^{1/2}t^{1/2}}, \tag{32}$$

where n is the number of transferred electrons, A is the surface area of the electrode, D_{ox} is the diffusion coefficient and C_{ox}^{*} is concentration of the reactant in bulk solution. Main point of the Cottrell equation is that when the current is under diffusion control the i vs $t^{-1/2}$ plot should be linear and its intersect zero. Thus at very long time frames the current should theoretically drop to zero although in reality this is not observed as at measurements of over around 30 s will start exhibiting natural convection. This is why in the experimental part the measurement time is limited to 10 s in order to avoid the onset of natural convection [3, 4].

When a potential step is applied the concentration of the reactant near the electrode surface changes as a function of time and the distance from the electrode surface x,

$$C_{\text{ox}}(x,t) = C_{\text{ox}}^{*}\text{erf}\left[\frac{x}{2(D_{\text{ox}}t)^{1/2}}\right]. \tag{33}$$

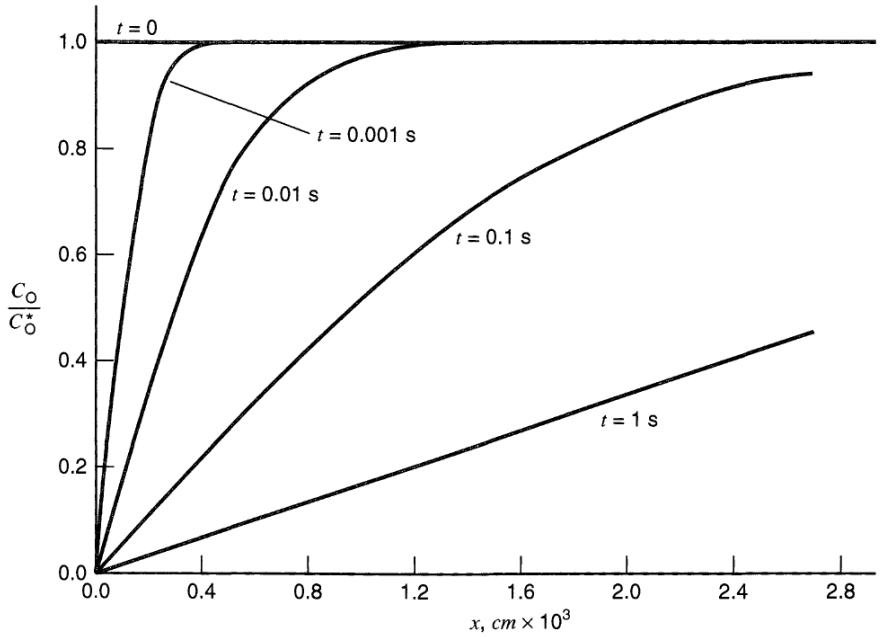

Figure 11: Concentration profiles of the reactant at different times after the applied potential. Figure by Bard and Faulkner [2].

The relative concentration of the reactant near the reactant when compared to the initial bulk concentration at different times t is presented in Figure 11. It can be seen that near the electrode surface the reactant concentration drops dramatically extremely quickly after the potential step. This drop of reactant concentration near the electrode can also be used to describe the thickness of the diffusion layer, which is defined by IUPAC as "The region in the vicinity of an electrode where the concentrations are different from their value in the bulk solution." [16], in the terms of $(D_{\text{ox}}t)^{1/2}$. The definition of the thickness varies by usage and user but the thickness of the diffusion layer is usually lower than $6(D_{\text{ox}}t)^{1/2}$, often settled around 1 to 2 times $(D_{\text{ox}}t)^{1/2}$. At distances greater than diffusion layer thickness the electrode's effect on concentration is negligible and no particles of the reactant can reach the electrode surface [2].

4.2 Cyclic voltammetry

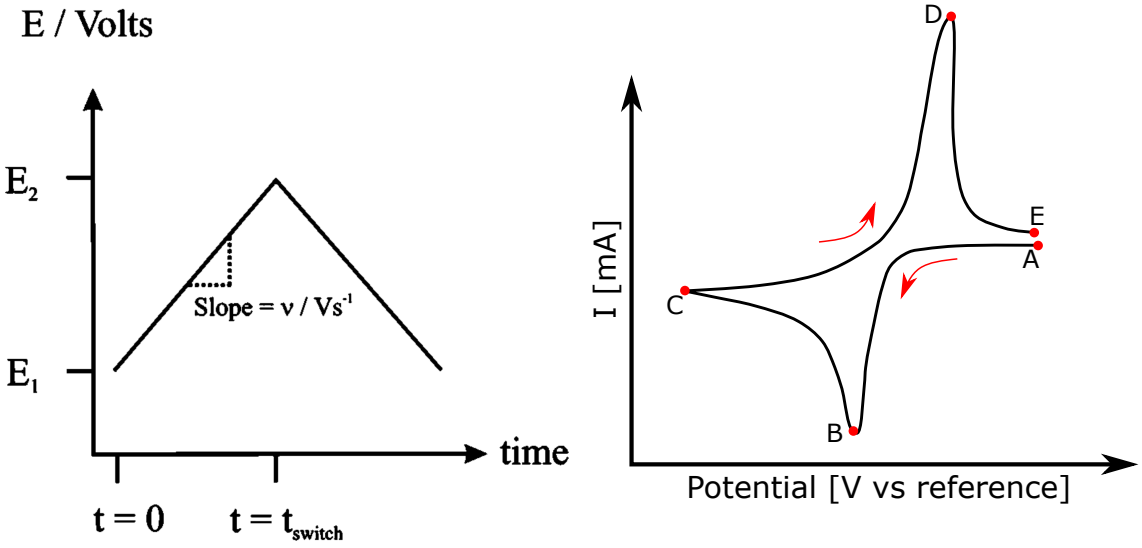

Figure 12: a) In cyclic voltammetry the potential is first linearly increased and then decreased. The slope of the curve is typically 50-100 mV/s. [6, 7] Image by Banks and Compton [6]. b) Typical voltammogram of an electrodeposition sweep.

The basic idea behind cyclic voltammetry is applying a potential to the working electrode that is time-dependent. The current flowing through the working electrode is recorded as a function of the applied potential. The applied potential starts to the working electrode starts at some value E_1 and then it's changed linearly to the potential E_2 and then the potential is again swept back to E_1. This has been depicted in Figure 12a. The initial potential E_1 is selected so that the chemical species of interest is not oxidized or reduced at the start of the potential sweep. Potential E_2 is selected so that the oxidation or reduction reaction of interest occurs within the potential difference between E_1 and E_2. This produces a graph known as a voltammogram and one charasteristic to electrodeposition is depicted in Figure 12b using the IUPAC convention. [6, 7]

In Figure 12b the potentials are scanned from point A to point C in what's typically known as negative or cathodic scan. During the cathodic scan the chemical

species of interest is reduced at the electrode. The cathodic current reaches its maximum at maximum concentration gradient at point B where the current is dictated by the diffusion of ions to the electrode surface. As more and more negative potentials are reached the chemical species keeps on reducing on the electrode surface, which starts forming a diffusion layer that inhibits the diffusion of new particles to the electrode surface causing a decrease in current between B and C. As point C is reached the direction of the scan is switched in what is known as positive or anodic scan. This time the concentration of the previously reduced species on the electrode is much higher and they start to oxidize back to oxidized species as the potential becomes more positive [7].

The scan rate, the slope of the potential in Figure 12a, determines how fast the potential is changed. Faster the scan rate is, higher currents are observed as faster scan rates cause the size of the diffusion layer to decrease. The scan rate is proportional to the square root of the peak current if the reaction is diffusion controlled. This however only applies to reactions that are electrochemically reversible. The reversibility of an reaction can be examined by using different scan rates and recording the peak currents. If plots of peak current vs square root of scan rate are not linear the reaction might only be quasi-reversible or the electron transfer is happening via another mechanism, such as through surface-adsorbed species [7].

5 Experiment

Palladium is quite unique element in that its ability to absorb hydrogen is much greater than most other metals and as such it's used widely in catalyzing hydrocarbons in e.g. automotive catalysts. The catalytic reactions are heavily affected by the crystal structure of palladium and there are many different ways to manufacture palladium structures, including but not limited to atomic layer deposition, sputtering and electrodeposition. Electrodeposition has a lot of benefits e.g. in production of Pd nanoparticles as it is relatively simple process that doesn't require expensive or very precise instruments or highly technical skills leading it to be very scalable when compared to atomic layer deposition or sputtering. The electrodeposition process along with the shape and size of the nanoparticles is also highly controllable because the system has many easily controlled variables such as electrodeposition potential, time, temperature and the composition of the electrolyte [17].

Most of the research done on palladium electrodeposition has been performed in aqueous solutions using light water (H_2O) and the motivation of this work is expand on that to perform electrodeposition in heavy water (D_2O) [17]. The main interest is in how using D_2O as the solvent and at different concentrations of acid affect the nucleation process. The experimental part of this study examines the effect of these two different parameters on the electrodeposition of palladium on pencil graphite electrode based on earlier research by M. Rezaei *et. al.* [18, 19], A. S. Fuentes *et. al.* [20] and T. Alemu *et. al.* [21].

5.1 Solution preparation

For this experiment two base solutions were made, both containing 7,5 mM $PdCl_2$ and 100 mM KCl in either D_2O (Armar Isotopes, 99,8%) or in ultrapure H_2O. Both base solutions were homogenized with an ultrasonicator until all of the $PdCl_2$ and KCl had been dissolved and a clear dark red/brown solution was formed. Other

Table 1: Different solutions used in the measurements.

Solution	Base	$PdCl_2$ [mM]	KCl [mM]	Sulphuric acid [mM]
1	D2O	7,5	100	0
2	D2O	7,5	100	10
3	D2O	7,5	100	100
4	D2O	7,5	100	1000
5	H2O	7,5	100	0
6	H2O	7,5	100	10
7	H2O	7,5	100	100
8	H2O	7,5	100	1000

solutions used in the experiment were made from these two solutions by adding either D_2SO_4 (Armar Isotopes, 99,5%) or H_2SO_4 (VWR, 95%) to their respective base solutions. Before being used for measurements, each solution was deaerated by bubbling with N_2 gas for 30 minutes in order to eliminate any dissolved oxygen [20].

In total eight different solutions were used in the measurements, later the cells containing these solutions are labeled based on the number of the solution. The cells and the concentrations of them are presented in Table 1.

5.2 Electrode preparation

For the working electrodes, common pencil graphite (Pentel Ain Stein 0,5 mm, B) was used. Before being used as electrodes they were cleaned by submerging them in 10% nitric acid solution for around 60 seconds and rinsed with deionized water afterwards and dried. Each piece of pencil graphite was used for only one measurement and only once. The surface area of the submerged part of the electrodes was 0,44 cm^2. For the counter electrode 0,5 mm diameter platinum wire with gold connector pin (Basi, MW-4130) was used and it was rinsed with deionized water

and dried before and after the solution was changed. The reference electrode used was one of the self-made 3 M KCl Ag/AgCl reference electrode with potential at +2,5 mV versus the laboratory master Ag/AgCl reference electrode (Fisherbrand accumet 13-620-53).

The reference electrodes were made by cutting a 4 cm piece of glass tube with diameter of 3 mm. A silver wire (0,25 mm diameter, 99,99%, Sigma-Aldrich) was cut to around 6 cm length and submerged in 0.1 M HNO_3 solution for 30 seconds and rinsed with deionized water. Then the silver wire was chlorinated in 0.1 M HCl solution with current of 125 μA for 1800 seconds so that around 2 cm of the wire was submerged in the HCl solution. This formed the AgCl layer on the wire after which it was inserted into the glass tube with a silica bead held in place by a heat-shrinking tube serving as a frit, which was then then filled with 3 M KCl solution and sealed with epoxy so that the non-chlorinated end of the silver wire was outside the glass tube.

5.3 Instruments and software

A potentiostat Gamry Instruments Reference 600+ was used to control and measure the potential of the working electrode with respect to the reference electrode while with recording the current passed between the working and counter electrodes. The software used to control the potentiostat was Gamry Instruments Framework version 7.8.2 build 7430.

For plots, fitting and data formatting OriginLab's Origin 2016 was used along with Python 3.8 with packages: Pandas, Matplotlib, NumPy and SciPy.

5.4 Experiments

Two types of experiments were performed using the setup described above. A cyclic voltammetry sweep was used to find the are potential range where Pd nucleation

and H/D absorption occurs for each specific solution. For this, a voltammetry sweep starting from +0,8 V with a scan rate of 20 mV/s. The potential at the negative end varied as H_2/D_2 evolution in more acidic solutions takes place at lower negative potentials and if the current was too high it risked causing too many H_2 bubbles in the porous pencil graphite, which could cause it to break. Two cycles were performed for each solution to check if the Pd nucleation peak would move right in the CV on the second sweep as described in literature.

After the Pd nucleation peak was identified, chronoamperometric measurements were performed in its potential region by taking a potential step from +0,7 V, which was initially kept for 30 seconds, to a lower potential for ten seconds before being returned to 0,7 V for 30 more seconds. For these measurements potentials ranging from +250 mV to -250 mV were used with steps size of 50 mV. It should be noted that for some measurements, mainly in Cell 6, the some of the more negative potentials were problematic and as such have been excluded from the results.

6 Results

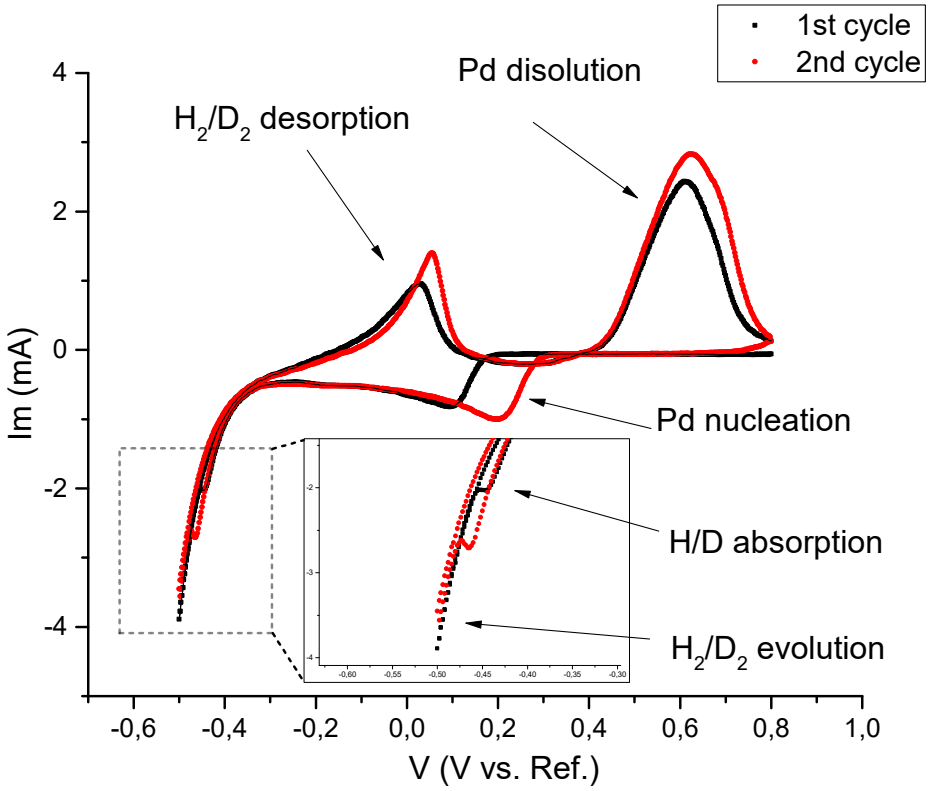

Figure 13: Cyclic voltammetry of Cell 3 containing 7,5 mM $PdCl_2$+ 100 mM KCl + 100 mM D_2SO_4 in D_2O. Palladium nucleation clearly starts earlier on the second cycle as there are some active sites leftover from the previous cycle on the electrode surface.

For all cells, the cyclic voltammetry measurements showed the expected characteristics, annotated in Figure 13, and confirmed the Pd nucleation peak starting earlier on second cycle when compared to the first cycle as reported by A. E. Alvarez and D.R. Salinas [13] and T. Alemu *et. al* [21]. According to Alvarez on the second scan there is some residual palladium deposits, which are not completely stripped off the electrode surface on the reverse scan leaving behind particles that act as active sites for the nucleation on subsequent sweeps, which require lower overpotential to be

activated.

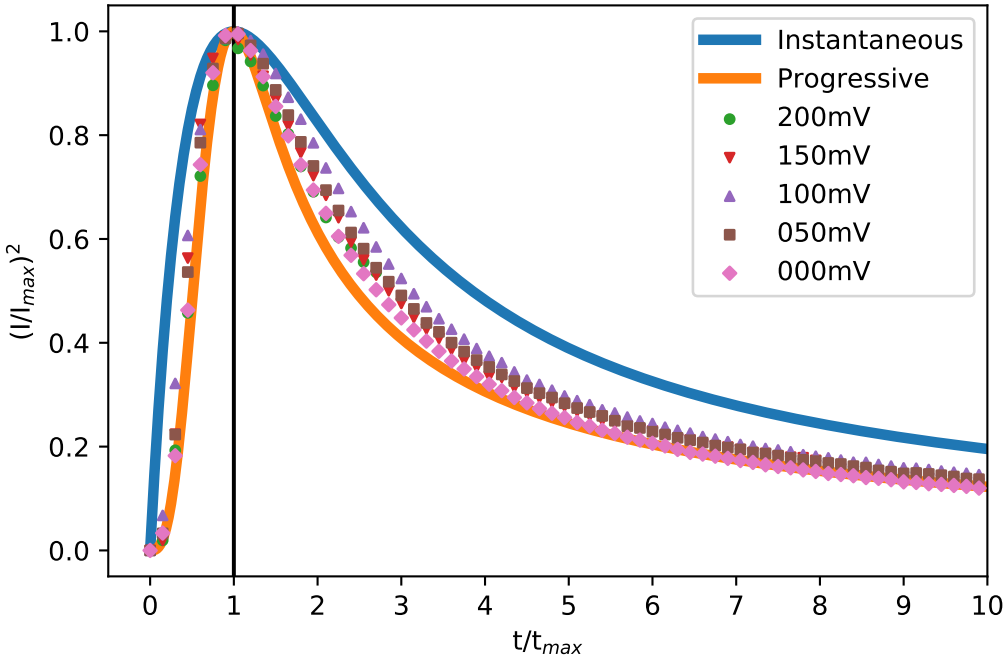

Figure 14: Dimensionless currents at 200 mV, 150 mV, 100 mV, 50 mV and 0 mV chronoamperometry steps for Cell 1.

To find out which one of the limiting cases of nucleation, progressive or instantaneous, was taking place in this system, the theory developed by B. Scharifker and G. Hills [12] was applied as discussed in section 3.3. This was done by scaling the data to a dimensionless form and then comparing it to the dimensionless equations of instantaneous (25) and progressive (26) nucleation. It should be noted that every measurement at more negative potentials was not usable as their peaks were cut off due to the potentiostat overloading during the first seconds of the applied chronoamperometric step.

As can be seen for Cell 1 in Figure 14, the nucleation mechanism corresponds more to progressive nucleation than instantaneous nucleation. This is observed in all measurements, the plots for cells 2-8 can be found in appendices 2-8. From this

the conclusion is made that in this experiment the acid added to the solution or switching H_2O to D_2O has no significant effect on the nucleation mechanism. It should be noted that in most literature both kinds of nucleation are present in varying degrees and that most of the time progressive nucleation has some instantaneous component and vice versa. These results can be compared to similar experiments by T. Alemu *et. al.* [21], who used glassy carbon electrode. In their experiments the nucleation was instantaneous in most cases, although when they fitted their data to the equations (25) and (26), they saw that the values where even greater than what instantaneous nucleation would predict. The authors attributed this to adsorption hydrogen ions on the electrode. When they performed the same experiments at much greater deposition potential and at $0,75$ mM solution, they observed that the nucleation process had changed to progressive nucleation process.

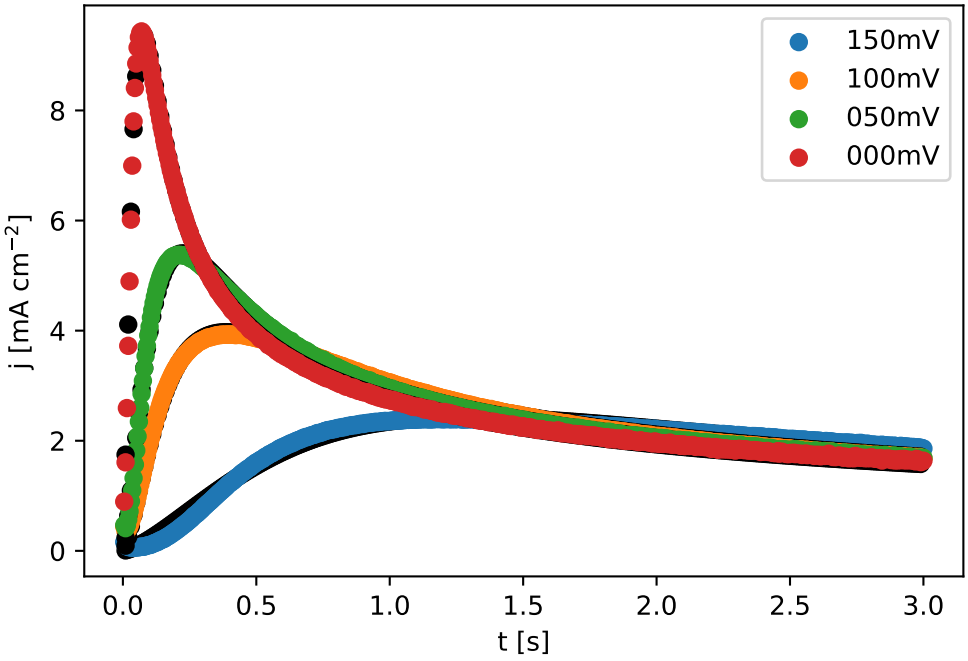

Figure 15: Chronoamperometric data for cell 1 for selected potentials along with fitted functions in black. Values of fitting function parameters A, N_0 and D are presented in Tables 2 and 3.

In section 3.3. the model by Heerman and Tarallo was discussed and that quantitative values could be obtained for nucleation constant per site A, number density of active sites N_0 and diffusion coefficient D by fitting the equation (21) to the chronoamperometric data. Reasonably good fits for most chronoamperometric measurements were obtained. For Cell 1 this is presented in Figure 15. Values for A, N_0 and D for cells containing D_2O and H_2O are presented in Tables 2 and 3, respectively along with the R^2 values of the fits.

Despite good fits, based on their R^2 values, some values at more negative overpotentials are many orders of magnitude off of their expected values. This is attributed to the fact that the potentiostat overloaded easily at negative overpotentials and didn't record the very high currents present at the top of the peak. The values for

cell 6 are also off by a lot. The reason for this is not known, although it should be noted that cell 6 had some troubles during the measurements where the current spiked up and down wildly at times.

Comparing to literature values presented by Alvarez and Satinas [13], who used slightly higher concentration and glassy carbon electrode with significantly smaller electrode surface area can be used to check whether the values are reasonable. In their measurements the diffusion coefficients varied from 8,8 $\times 10^6$ cm s^{-1} to 9,3 $\times 10^6$ cm s^{-1}, which are slightly lower than the ones in these experiments. While D_2O should theoretically have a slightly smaller diffusion coefficient, due to its higher viscosity [22, 23], than H_2O, no clear differences in D_2O and H_2O solutions' diffusion coefficients leaving these observations thus far unexplained.

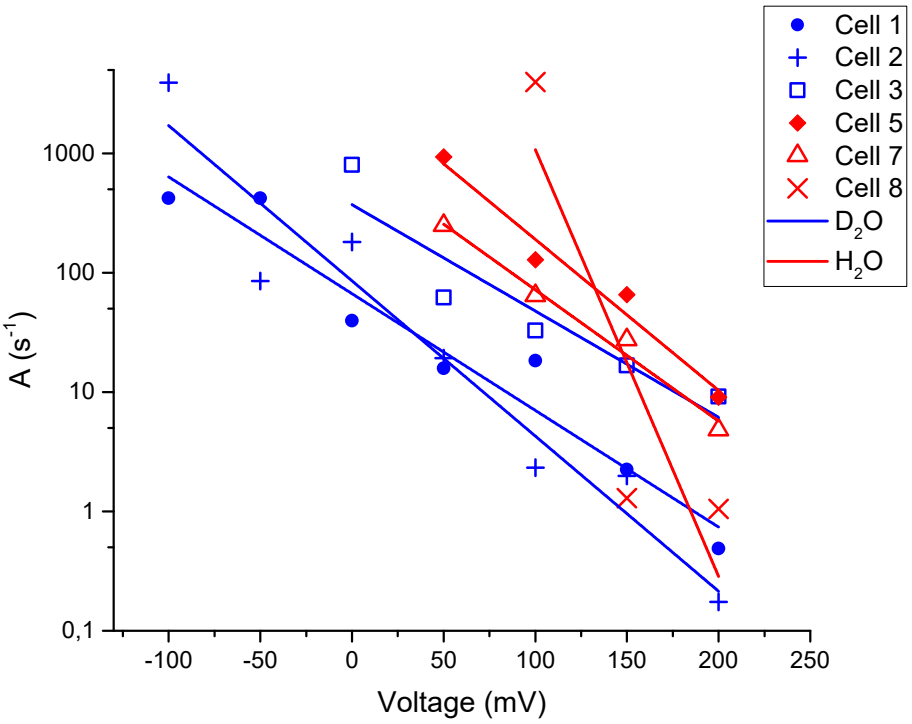

Figure 16: Values of nucleation rate constant per site A as a function of the applied step voltage for cells 1, 2, 3, 5, 7 and 8 with linear fitting color coded based on whether the solution was D_2O or H_2O based.

For nucleation constant per site A Alvarez and Satinas report a decreasing linear relationship between logarithm of A and the overpotential which has been presented for this experiment in Figure 16. Most of the negative overpotentials have been left out as their values are orders of magnitude too large to be considered reasonable. For all but Cells 4 and 6 the dependence of nucleation rate constant with respect to voltage seems to match the one reported by Alvarez and Satinas. For Cells 4 and 6 there is no clear explanation as to why their values are wildly different from others and why Cell 4 sees the linear fit trending upwards instead of downwards. If these cells are ignored as experimental errors it seems that the values of A are generally smaller for solutions containing D_2O when compared to H_2O solutions. This should be studied further as it's not clear if D_2O affects the nucleation constant per site. Heavy water solutions are not studied nearly as widely as light water solutions, which are the norm, and as such this might be an interesting new phenomenon which warrants additional experimentation.

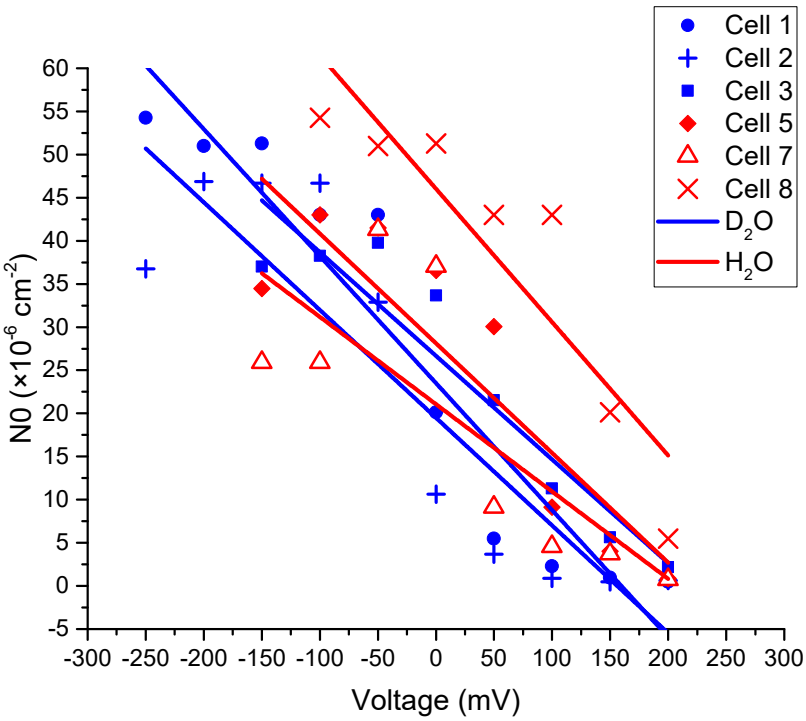

Figure 17: Number densities of active sites N_0 for cells 1, 2, 3, 5, 7 and 8 as function of overpotential along with linear fitting.

Number density of active sites N_0 seems to grow as the potential step becomes larger as can be seen in Figure 17 and this relationship seems to be linear in nature. No clear trend can been seen between cells containing D_2O or H_2O. It sounds logical that as the potential difference is increased more of the sites are activated becoming active sites. This matches the results by T. Alemu *et. al.* [21] who saw similar results of greater number of active sites at greater potential differences. When they observed instantaneous nucleation the values for number density of active sites were slightly higher owing this to the effect of the nucleation mechanism.

Table 2: Values for A, N_0 and D for different D_2O cells at different potentials. Only voltages where reasonably good R-values were obtained are shown and used in the plots.

Cell	U [mV]	A [s^{-1}]	N_0 [$\times 10^{-6}$ cm^{-2}]	D [$\times 10^{6}$ cm^{-1}]	R^2
1	200	0,490	0,50	11,5	0,996
1	150	2,25	0,96	13,9	0,994
1	100	18,3	2,28	13,5	0,994
1	50	15,8	5,48	12,7	0,997
1	0	39,7	20,1	11,7	0,996
1	-50	421,0	43,0	12,1	0,996
1	-100	421,0	43,0	12,7	0,995
1	-150	$7{,}19\times10^{9}$	51,3	12,3	0,992
1	-200	$1{,}54\times10^{11}$	51,0	12,5	0,989
1	-250	$5{,}78\times10^{10}$	54,3	12,1	0,989
2	200	0,17	0,64	9,60	0,987
2	150	1,99	0,50	14,9	0,995
2	100	2,33	0,88	14,6	0,995
2	50	19,3	3,67	14,1	0,991
2	0	181,0	10,6	14,0	0,991
2	-50	85,2	32,9	12,0	0,996
2	-100	3920	46,7	12,5	0,995
2	-150	3920	46,7	13,0	0,993
2	-200	$6{,}90\times10^{7}$	46,9	13,0	0,989
2	-250	$2{,}21\times10^{10}$	36,8	14,6	0,989
3	100	9,15	2,18	12,6	0,960
3	50	16,7	5,65	13,7	0,979
3	0	32,8	11,3	14,2	0,989
3	-50	61,9	21,5	13,1	0,996
3	-100	803,0	33,7	14,2	0,996
3	-150	$1{,}10\times10^{10}$	39,8	14,1	0,989
3	-200	$1{,}65\times10^{10}$	38,3	14,3	0,990
3	-250	$3{,}33\times10^{10}$	37,0	14,6	0,990
4	100	0,316	9,57	12,0	0,999
4	50	0,130	787,0	10,1	0,991
4	0	0,100	$3{,}55\times10^{4}$	8,85	0,994
4	-50	0,0580	$1{,}40\times10^{5}$	8,60	0,961
4	-100	0,0520	$1{,}75\times10^{5}$	8,21	0,948
4	-150	0,0520	$1{,}75\times10^{5}$	8,34	0,947
4	-200	0,0520	$1{,}75\times10^{5}$	8,69	0,947
4	-250	0,0490	$2{,}11\times10^{5}$	7,97	0,947

Table 3: Values for A, N_0 and D for different H_2O cells at different potentials. Only voltages where reasonably good R-values were obtained are shown and used in the plots.

Cell	U [mV]	A [s^{-1}]	N_0 [$\times 10^{-6}$ cm^{-2}]	D [$\times 10^{6}$ cm^{-1}]	R^2
5	100	$4{,}14\times10^{5}$	0,84	16,3	0,937
5	50	9,05	4,02	14,6	0,991
5	0	65,6	9,14	14,5	0,993
5	-50	128,0	30,0	14,5	0,994
5	-100	932,0	36,6	14,0	0,994
5	-150	$7{,}18\times10^{9}$	41,5	13,7	0,989
5	-200	$1{,}71\times10^{11}$	44,0	13,5	0,987
5	-250	$1{,}43\times10^{12}$	34,5	15,1	0,987
6	200	0,12	0,14	8,98	0,951
6	150	$6{,}75\times10^{-4}$	329,0	12,8	0,993
6	100	$1{,}54\times10^{-3}$	1280	13,5	0,994
6	50	$1{,}63\times10^{-3}$	$2{,}11\times10^{4}$	11,2	0,995
6	0	$2{,}19\times10^{-3}$	$1{,}19\times10^{5}$	10,4	0,995
6	-50	$2{,}19\times10^{-3}$	$1{,}19\times10^{5}$	10,4	0,995
7	100	4,83	0,74	16,8	0,995
7	50	27,5	3,73	15,1	0,993
7	0	64,3	4,56	15,3	0,988
7	-50	248,0	9,11	17,2	0,989
7	-100	$2{,}89\times10^{7}$	37,0	13,9	0,994
7	-150	$1{,}35\times10^{10}$	41,3	13,7	0,992
7	-200	$1{,}15\times10^{12}$	25,9	17,2	0,994
7	-250	$1{,}15\times10^{12}$	25,9	18,5	0,982
8	100	1,05	5,48	14,5	0,997
8	50	1,29	20,1	12,6	0,983
8	0	$6{,}79\times10^{5}$	43,0	12,4	0,968
8	-50	$3{,}95\times10^{6}$	43,0	11,4	0,986
8	-100	3970	51,3	10,6	0,994
8	-150	$7{,}95\times10^{9}$	51,0	12,6	0,988
8	-200	$6{,}34\times10^{10}$	54,3	13,3	0,991
8	-250	$1{,}17\times10^{12}$	0,64	15,3	0,977

7 Conclusions

This Master's thesis introduces the basic concepts of electrochemistry starting from components of electochemical cells and discusses the theoretical background of the processes behind the reactions within electrochemical cells. Then two of the most common electrochemical measurements, chronoamperometry and cyclic voltammetry is introduced and then applied in experimental section where the effect of acidity and isotopes of hydrogen in water are examined in electrodeposition of palladium on pencil graphite working electrode. The data is examined quantitatively and qualitatively and following conclusions are made: 1) In this system nucleation of palladium was dominated by progressive nucleation mechanism. 2) Current profile for chronoamperometric measurements followed the theory by Heerman and Tarallo [14] and from it values for nucleation constant per site, number density of active sites and diffusion coefficient were acquired by non-linear curve fitting. 3) Nucleation constants per site mostly had the trend described in literature with the caveat that its values tended to be slightly smaller for solutions of D_2O when compared the values of solutions in H_2O. This warrants additional experimentation. 4) Isotope effects for diffusion coefficient or number density of active sites were not observed. Number density of active sites generally increases as the potential step becomes larger which matches the physical intuition of the system and literary sources.

Overall the topics covered in this study warrant additional experimentation and research and it should be noted that electrochemical reactions using heavy water as the solvent have not been studied as nearly widely when compared to light water solvents. These experiments were also unable to study the H_2/D_2 absorption at the same potential region as palladium deposition as the H_2/D_2 absorption occurred only at much greater negative potentials when compared to the palladium deposition region. This could be studied by utilizing even more acidic solutions.

References

[1] Lasse Murtomäki et al. *Sähkökemia*. Suomi: [Teknillinen korkeakoulu, kirjasto], 2009. ISBN: 978-952-248-072-9.

[2] Allen J. Bard and Larry R. Faulkner. *Electrochemical Methods: Fundamentals and Applications*. 2nd. Wiley, 2001.

[3] Cynthia Zoski. *Handbook of Electrochemistry*. Jan. 2007. ISBN: 9780444519580. DOI: 10.1016/B978-0-444-51958-0.X5000-9.

[4] Allen J. Bard and Larry R. Faulkner. *Electrochemical Methods: Fundamentals and Applications*. Wiley, 1980. ISBN: 9780471055426.

[5] C.H. Hamann, A. Hamnett, and W. Vielstich. *Electrochemistry*. Wiley, 2007. ISBN: 9783527310692. URL: https://books.google.fi/books?id=EXljvgAACAAJ.

[6] Richard Compton and Craig Banks. *Understanding Voltammetry*. World Scientific Publishing Europe Ltd., Aug. 2018, p. 439. ISBN: 978-1-78634-526-4. DOI: 10.1142/q0155.

[7] Noémie Elgrishi et al. "A Practical Beginner's Guide to Cyclic Voltammetry". In: *Journal of Chemical Education* 95.2 (2018), pp. 197–206. DOI: 10.1021/acs.jchemed.7b00361. eprint: https://doi.org/10.1021/acs.jchemed.7b00361.

[8] John Newman and Karen Thomas-Alyea. *Electrochemical Systems*. John Wiley & Sons, Ltd, 2004. ISBN: 9780471477563.

[9] Weiwei Cai et al. "2 - Electrode Kinetics of Electron-Transfer Reaction and Reactant Transport in Electrolyte Solution". In: *Rotating Electrode Methods and Oxygen Reduction Electrocatalysts*. Ed. by Wei Xing, Geping Yin, and Jiujun Zhang. Amsterdam: Elsevier, 2014, pp. 33–65. ISBN: 978-0-444-63278-4. DOI: https://doi.org/10.1016/B978-0-444-63278-4.00002-1.

[10] Hugh D. Young and Roger A. Freedman. *Sears and Zemansky's University Physics: With Modern Physics*. Addison-Wesley, 2012. ISBN: 9780321696854.

[11] Vladimir S. Bagotsky. "Polarization of Electrodes". In: *Fundamentals of Electrochemistry*. John Wiley & Sons, Ltd, 2005. Chap. 6, pp. 79–98. ISBN: 9780471741992. DOI: https://doi.org/10.1002/047174199X.ch6.

[12] Benjamin Scharifker and Graham Hills. "Theoretical and experimental studies of multiple nucleation". In: *Electrochimica Acta* 28 (July 1983), pp. 879–889. DOI: 10.1016/0013-4686(83)85163-9.

[13] A.E. Alvarez and D.R. Salinas. "Formation of Cu/Pd bimetallic crystals by electrochemical deposition". In: *Electrochimica Acta* 55.11 (2010), pp. 3714–3720. ISSN: 0013-4686. DOI: https://doi.org/10.1016/j.electacta.2010.01.076.

[14] Luc Heerman and Anthony Tarallo. "Theory of the chronoamperometric transient for electrochemical nucleation with diffusion-controlled growth". In: *Journal of Electroanalytical Chemistry* 470 (July 1999), pp. 70–76. DOI: 10.1016/S0022-0728(99)00221-1.

[15] D.J. Lomax, I.A. Kinloch, and R.A.W. Dryfe. "Au electrodeposition on carbon materials". In: *Proceedings of the IEEE Conference on Nanotechnology* (2012). cited By 2. DOI: 10.1109/NANO.2012.6322218.

[16] International Union of Pure and Applied Chemistry. *IUPAC Compendium of Chemical Terminology – The Gold Book*. 2009. URL: http://goldbook.iupac.org/.

[17] Haytham E. M. Hussein et al. "Controlling palladium morphology in electrodeposition from nanoparticles to dendrites via the use of mixed solvents". In: *Nanoscale* 12 (42 2020), pp. 21757–21769. DOI: 10.1039/D0NR05630H. URL: http://dx.doi.org/10.1039/D0NR05630H.

[18] Milad Rezaei, S.Hadi Tabaian, and Davoud Haghshenas Fatmehsari. "Nucleation and growth of Pd nanoparticles during electrocrystallization on pencil graphite". In: *Electrochimica Acta - ELECTROCHIM ACTA* 59 (Jan. 2011). DOI: 10.1016/j.electacta.2011.10.081.

[19] Milad Rezaei, S.Hadi Tabaian, and Davoud Haghshenas Fatmehsari. "Electrochemical nucleation of palladium on graphene: A kinetic study with an emphasis on hydrogen co-reduction". In: *Electrochimica Acta* 87 (Jan. 2013), pp. 381–387. DOI: 10.1016/j.electacta.2012.09.092.

[20] Ana Fuentes et al. "Pd Nucleation and Growth Mechanism Deposited on Different Substrates". In: *Procedia Materials Science* 8 (Dec. 2015), pp. 541–550. DOI: 10.1016/j.mspro.2015.04.107.

[21] Tibebu Alemu, Birhanu Desalegn Assresahegn, and Tesfaye Soreta. "Tuning the Initial Electronucleation Mechanism of Palladium on Glassy Carbon Electrode". In: *Portugaliae Electrochimica Acta* 32 (Jan. 2014), pp. 21–33. DOI: 10.4152/pea.201401021.

[22] Robert C. Hardy and Robert L. Cottington. "Viscosity of deuterium oxide and water in the range 5 to 125 C". In: *Journal of research of the National Bureau of Standards* 42 (1949), p. 573.

[23] Albert Einstein. "Über die von der molekularkinetischen Theorie der Wärme geforderte Bewegung von in ruhenden Flüssigkeiten suspendierten Teilchen". In: *Annalen der Physik* 322.8 (1905), pp. 549–560. DOI: https://doi.org/10.1002/andp.19053220806.

8 Appendix

1. Python program `CV_and_CA_data.py` was used for data manipulation, plotting and for fitting curves in this thesis.

2. Chronoamperometric dimensionless data of cell 2 and functions for instantaneous and progressive nucleation.

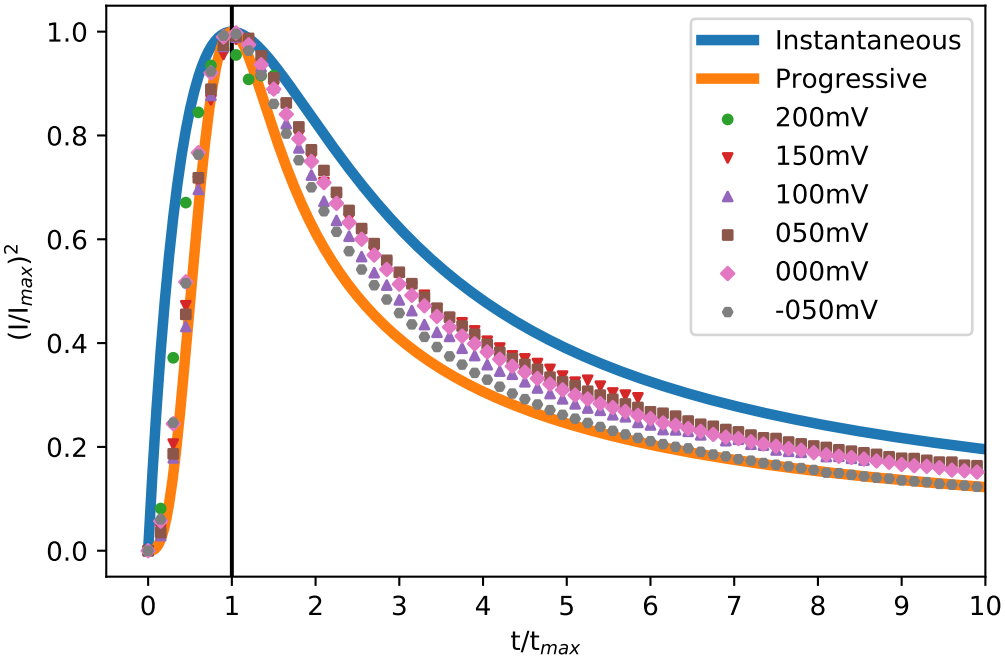

3. Chronoamperometric dimensionless data of cell 3 and functions for instantaneous and progressive nucleation

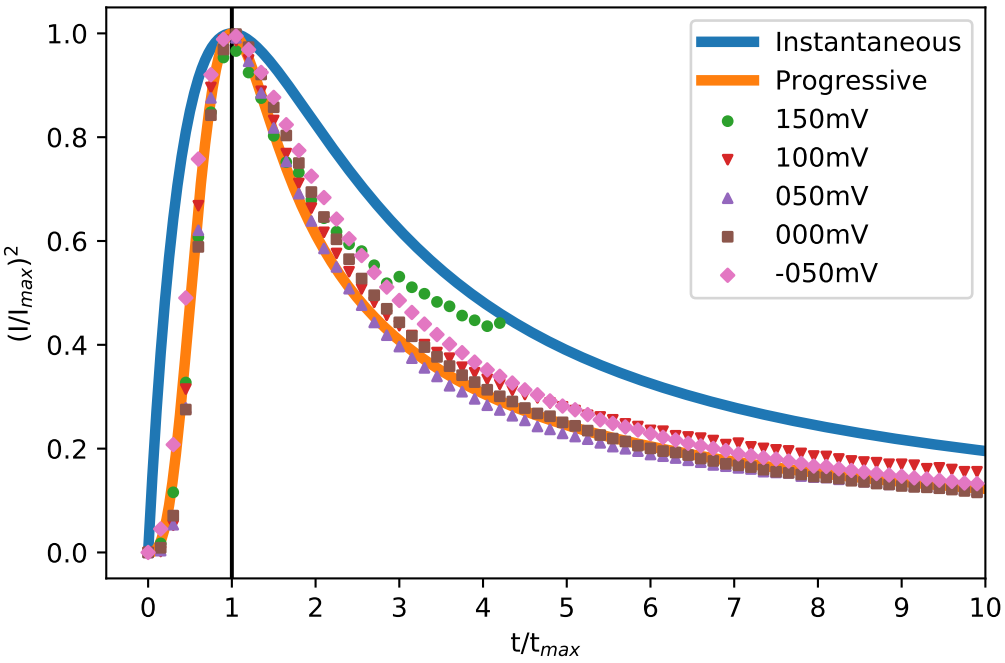

4. Chronoamperometric dimensionless data of cell 4 and functions for instantaneous and progressive nucleation

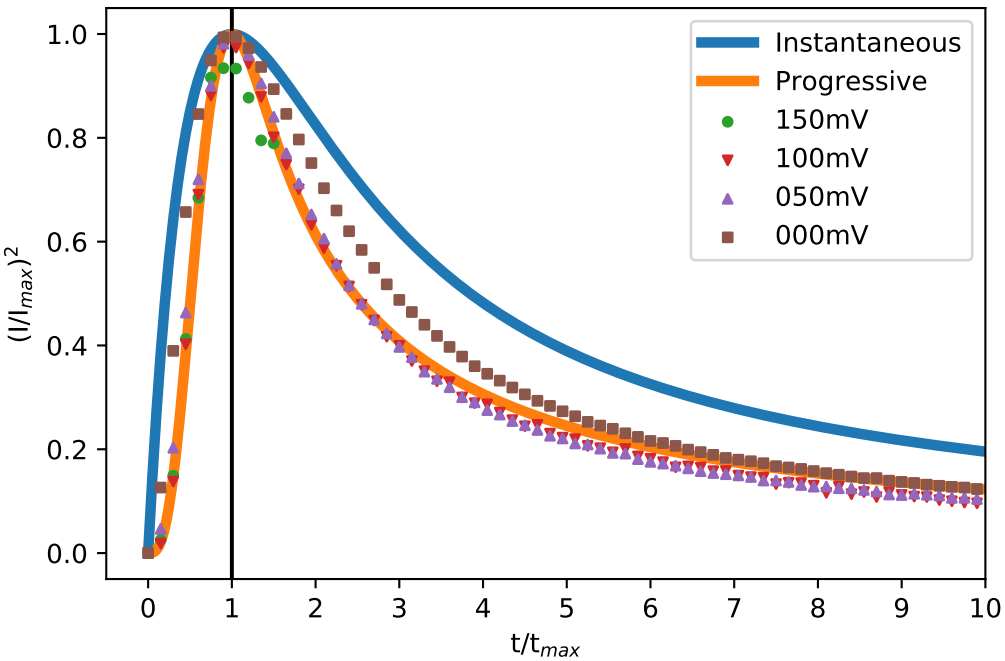

5. Chronoamperometric dimensionless data of cell 5 and functions for instantaneous and progressive nucleation

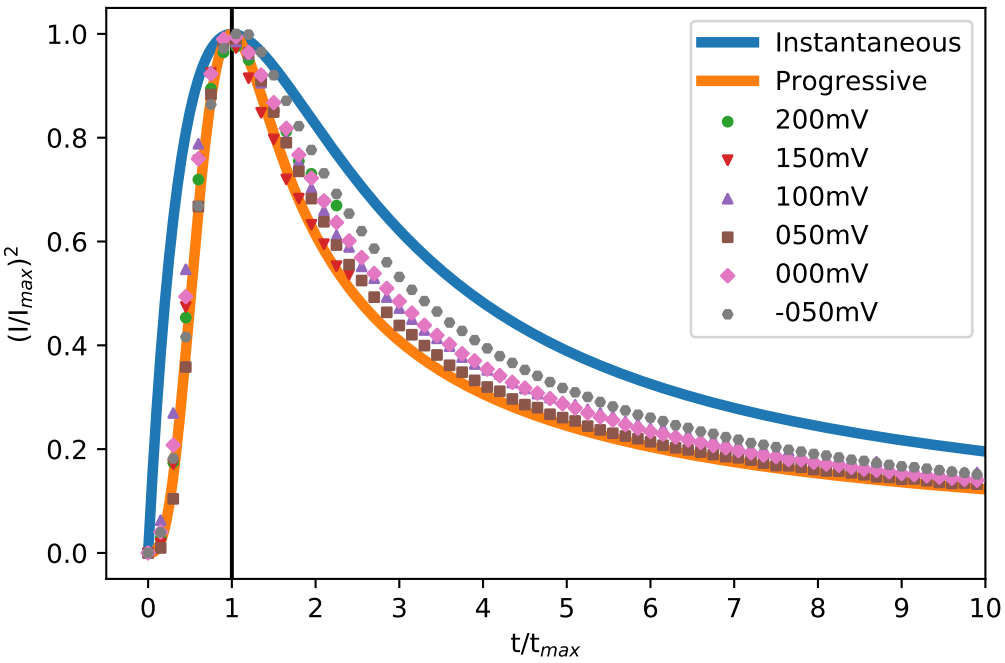

6. Chronoamperometric dimensionless data of cell 6 and functions for instantaneous and progressive nucleation

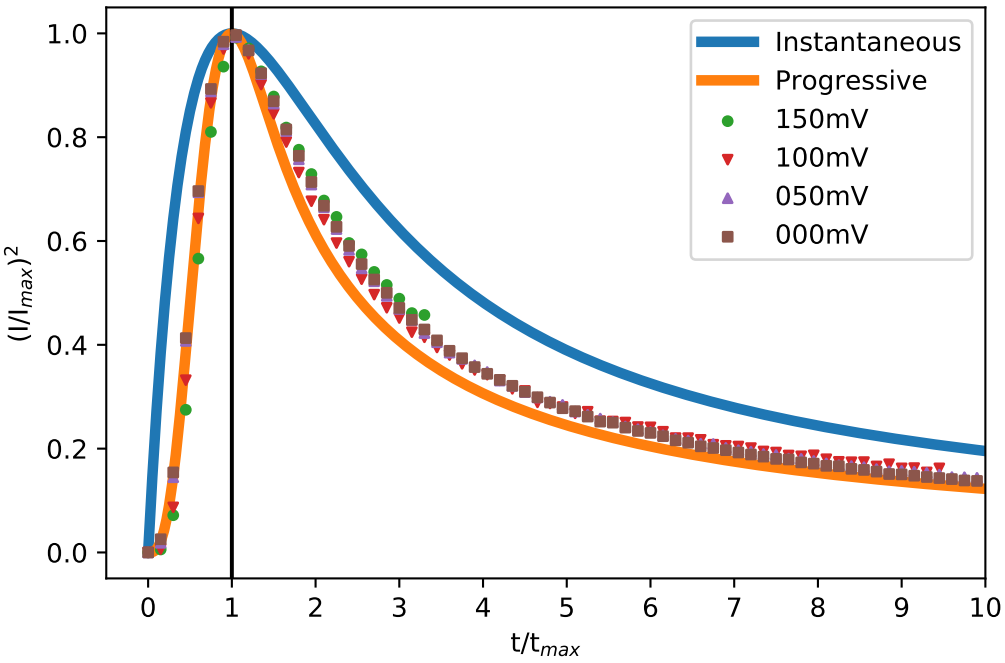

7. Chronoamperometric dimensionless data of cell 7 and functions for instantaneous and progressive nucleation

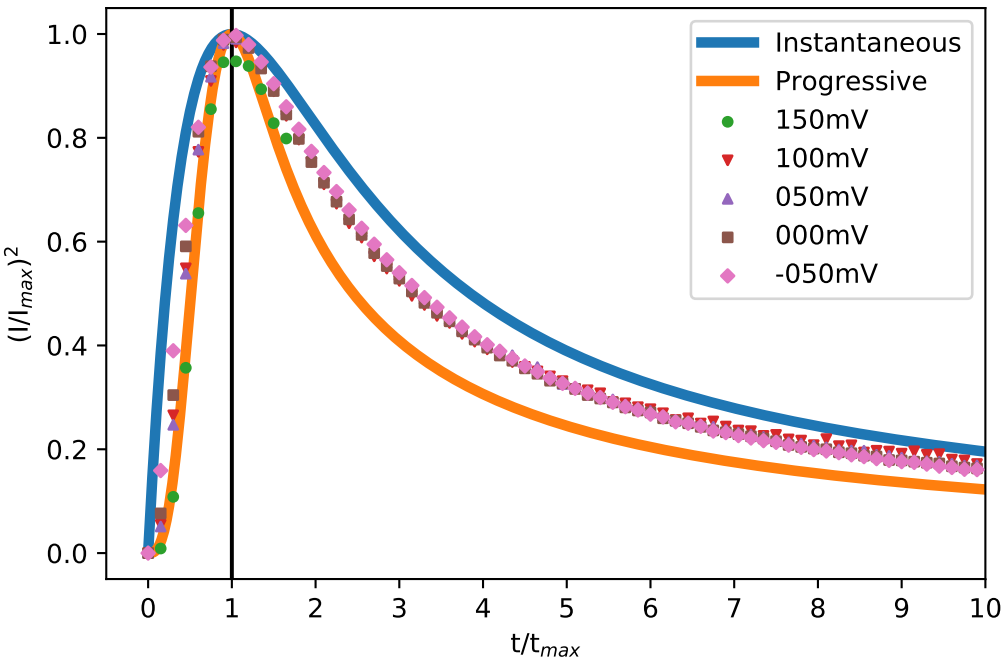

8. Chronoamperometric dimensionless data of cell 8 and functions for instantaneous and progressive nucleation